
TENSOR-BASED EMPIRICAL INTERPOLATION METHOD, AND ITS APPLICATION IN MODEL REDUCTION

Brij Nandan Tripathi

Department of Electronics and Electrical Engineering
Indian Institute of Technology Guwahati
Assam, India
brij18@iitg.ac.in

Hanumant Singh Shekhawat

Department of Electronics and Electrical Engineering
Indian Institute of Technology Guwahati
Assam, India
h.s.shekhawat@iitg.ac.in

October 30, 2024

ABSTRACT

In general, matrix or tensor-valued functions are approximated using the method developed for vector-valued functions by transforming the matrix-valued function into vector form. This paper proposes a tensor-based interpolation method to approximate a matrix-valued function without transforming it into the vector form. The tensor-based technique has the advantage of reducing offline and online computation without sacrificing much accuracy. The proposed method is an extension of the empirical interpolation method (EIM) for tensor bases. This paper presents a necessary theoretical framework to understand the method's functioning and limitations. Our mathematical analysis establishes a key characteristic of the proposed method: it consistently generates interpolation points in the form of a rectangular grid. This observation underscores a fundamental limitation that applies to any matrix-based approach relying on widely used techniques like EIM or DEIM method. It has also been theoretically shown that the proposed method is equivalent to the DEIM method applied in each direction due to the rectangular grid structure of the interpolation points. The application of the proposed method is shown in the model reduction of the semi-linear matrix differential equation. We have compared the approximation result of our proposed method with the DEIM method used to approximate a vector-valued function. The comparison result shows that the proposed method takes less time, albeit with a minor compromise with accuracy.

1 Introduction

The complexity of dynamical systems in science and engineering has increased dramatically due to the ever-increasing demand for accuracy. Today's large-scale dynamical system requires enormous computational power for numerical simulation. Model order reduction (MOR) helps generate a reduced model that accurately represents dynamics of interest and requires less computation time. Application of MOR can be found in many areas, such as electrical grid [2], biological system [3], and CFD-based modeling and control [39]. The application of MOR is widespread across various domains, including the electrical grid [2], biological systems [3], CFD-based modeling and control [39], and numerous others [47, 46, 45, 44].

The MOR works well in many areas due to the fact that the solution is attracted to a low dimensional manifold, though it is represented in very high-dimension in full order model (FOM) [15]. Hence, the initial stage of Model Order Reduction (MOR) involves identifying the low-dimensional manifold that approximately contains the solution trajectories. If we regard this low-dimensional space as a linear subspace, several widely recognized techniques can be mentioned, such as rational interpolation [26], the reduced basis method [25], and proper orthogonal decomposition (POD) [8], [27], among others. POD, initially introduced in the context of turbulent flow [8], is an empirical method closely linked to principal component analysis (PCA). Subsequently, the system is projected onto the low-dimensional space usually with galerkin method to reduce the system dimensionality [27, 28]. The POD-Galerkin method does effective model reduction for linear and bi-linear systems [15]. In the case of general non-linear systems, the dependence on the dimensionality of the full-order system persists. To alleviate this dependency on the FOM dimension,

several methods have been proposed, such as [13, 11, 15, 10, 49, 48]. The masked projection[10], gauss newton with approximated tensor (GNAT) [11] and missing point estimation [13] have used the concept of gappy POD, whereas discrete empirical interpolation method (DEIM) [15] is an interpolation-based method. DEIM is a discrete version of the empirical interpolation method (EIM) [14], which generates interpolation points from a given basis set to approximate the function. This approximated function is then employed in the POD - Galerkin reduced model to eliminate the reliance on the FOM dimension. Different up-gradation and variations of DEIM have been proposed to perform better in different applications, resulting in Localised DEIM [18], Randomized DEIM [29], matrix DEIM [19], and Q-DEIM [17].

All extensions of DEIM work on vector-valued functions, but in some applications, non-linearity may be a matrix-valued function. For example, non-linearity in the system arises from discretizing the three-dimensional partial differential equation (PDE). Here, a three-dimensional PDE pertains to an equation with two spatial independent variables and one temporal or parameter independent variable. So, to calculate non-linear terms efficiently in POD reduced system, an interpolation-based approximation of the large matrix-valued function is required. This problem can also be solved by applying DEIM after vectorizing the matrix-valued function into a vector-valued function. However, this is computationally inefficient for functions with a large matrix as output. In this paper, we present a theoretical foundation for the approximation of matrix-valued functions, which is an extension of EIM (Empirical Interpolation Method). Although a few researchers have worked in this direction [38, 43], a proper theoretical framework is missing to the best of our knowledge. The proposed framework is necessary to answer a lot of questions related to the functioning and limitations of the method. There are two important theoretical questions: The first is how a discrete matrix version of EIM relates to matrix DEIM proposed in [38]. We have mathematically proved the equivalence. The second question is more related to the interpolation points. Generally, we expect the points selected by any matrix version of EIM to be the sampling points anywhere on the grid. However, we have observed that this is not the case. Mathematically, we have shown in the paper that for tensor basis or rank one matrix basis, the proposed method selects interpolation points always on a rectangular grid. For instance, if we want to approximate the matrix-valued function with 24 interpolation points, it selects four rows, and from those selected four rows, it selects six elements such that it forms a rectangular grid. The proposed method always selects an equal number of elements from selected rows. The strategy of removing non-zero entries [40] can be easily adopted in the proposed method. We have also shown the application of the proposed framework in the model reduction of matrix and vector differential equations.

The rest of the paper is organized as follows: The interpolation-based approximation procedure of the matrix-valued function is explained in Section 2, followed by the algorithm to select the interpolation points and its analysis results in Section 3. Application of the proposed approximation in model reduction of non-linear dynamical system and numerical simulation of the same are described in Section 4.

1.1 Notations

In this section, we have defined a few notations which are used in this work. An operator vec is used to vectorize a matrix column-wise. Suppose $A = [a_1 \ a_2 \ a_3 \ \dots \ a_n]$ is a matrix, its vectorized form is denoted as $vec(A) = [a_1^T \ a_2^T \ a_3^T \ \dots \ a_n^T]^T$ and vec_{mn}^{-1} maps a vector with mn elements into $m \times n$ matrix. Moreover, if $a = [a_1^T \ a_2^T \ a_3^T \ \dots \ a_n^T]^T$ is a vector with mn elements, vec_{mn}^{-1} is equal to the matrix $[a_1 \ a_2 \ a_3 \ \dots \ a_n]$ with m rows and n columns. The symbols \otimes_{kr} , \otimes_K , and \otimes represent column-wise Khatri-Rao product, Kronecker product, and tensor product, respectively. e_k denotes the k^{th} column of identity matrix. Let $A = [a_{ij}] \in \mathbb{R}^{m \times n}$ be a matrix. Then, the diagonal extraction operator $vecd$ of A is defined below

$$vecd(A) = [a_{11} \ a_{22} \ \dots \ a_{mm}]^T \quad (1)$$

2 Non-linear matrix approximation using tensors

This section describes an approximation procedure for the non-linear matrix $A(x)$. The conventional matrix flattening method [40, 41] is not considered here because it requires more computation (in the offline/online stage) and is unsuitable for large matrices, as mentioned in [50]. The proposed approach is inspired by the Empirical Interpolation Method (EIM) [14] and the Discrete Empirical Interpolation Method [15], and develops two-dimensional approximation without matrix flattening. This can be easily extended for higher dimensions.

Let $U_i \in \mathbb{R}^{n_1 \times n_2}$ for all $i \in \{1, 2, \dots, m_1 m_2\}$ are linearly independent matrices, where $m_1 \leq n_1, m_2 \leq n_2 \in \mathbb{N}$. The projection of matrix $A(t) \in \mathbb{R}^{n_1 \times n_2}$ onto the space spanned by U_i 's is given by:

$$A(t) \approx \hat{A}(t) = U_1 c_1(t) + \dots + U_{m_1 m_2} c_{m_1 m_2}(t) \quad (2)$$

where, $c_i(t) \in \mathbb{R}$, U_i 's are the POD bases of the matrix $A(t)$ and $\hat{A}(t)$ represents the approximated matrix on $m_1 m_2$ number of POD bases. Moreover (2) can be expressed by defining projection operator $\mathcal{U} : \mathbb{R}^{m_1 \times m_2} \rightarrow \mathbb{R}^{n_1 \times n_2}$ as,

$$\hat{A}(t) = \mathcal{U}c(t) \quad (3)$$

where,

$$c(t) = \text{vec}_{m_1 m_2}^{-1} [c_1(t) \quad c_2(t) \quad \dots \quad c_{m_1 m_2}(t)] \quad (4)$$

$$\mathcal{U}c(t) = \sum_{i=1}^{m_1 m_2} \langle c(t), \text{vec}_{m_1 m_2}^{-1}(e_i) \rangle U_i \quad (5)$$

where, e_i is i^{th} column of identity matrix $I \in \mathbb{R}^{m_1 m_2 \times m_1 m_2}$.

Since our approximation method is an interpolation-based method, to determine the interpolation points from a given set of sampling points, we utilize the masking operator, defined as follows:

Definition 1. A mask is an operator from $\mathbb{R}^{n_1 \times n_2}$ to $\mathbb{R}^{m_1 \times m_2}$. For $X = [x_{ij}]_{(i=1, j=1)}^{(n_1, n_2)}$, it is defined as

$$M(X) = \begin{bmatrix} x_{i_1 j_1} & \dots & x_{i_{m_1} j_{m_1}} \\ x_{i_{m_1+1} j_{m_1+1}} & \dots & x_{i_{2m_1} j_{2m_1}} \\ \vdots & \dots & \vdots \\ x_{i_{(m_2-1)m_1+1} j_{(m_2-1)m_1+1}} & \dots & x_{i_{m_1 m_2} j_{m_1 m_2}} \end{bmatrix} \quad (6)$$

for given indices $i_1, i_2, \dots, i_{m_1 m_2}$ and $j_1, j_2, \dots, j_{m_1 m_2}$.

The mask can be easily redefined such that it maps $\mathbb{R}^{n_1 \times n_2}$ to any space which is isomorphic to $\mathbb{R}^{m_1 \times m_2}$. It is trivial that

$$\text{vec}(MX) = P^T \text{vec}(X) \quad (7)$$

where,

$$P = [e_{i_1+n_1(j_1-1)} \quad e_{i_2+n_1(j_2-1)} \quad \dots \quad e_{i_{m_1 m_2}+n_1(j_{m_1 m_2}-1)}]$$

where, $e_k \in \mathbb{R}^{n_1 n_2}$ are the standard unit vectors.

An approximation of $A(t)$ can be obtained by using the following method, which is an extension of the approximation method used in [15] for matrices. Suppose $A(t) \in \mathbb{R}^{n_1 \times n_2}$, $\hat{A}(t) \in \mathbb{R}^{n_1 \times n_2}$, $t \in \mathbb{R}$ and $M : \mathbb{R}^{n_1 \times n_2} \rightarrow \mathbb{R}^{m_1 \times m_2}$ denote original matrix, approximated matrix, time, and mask operator, respectively. Equation (3) is an over-determined set due to fewer unknowns than the number of equations. Given a mask M , we use the following consistency condition

$$M(\hat{A}(t)) = M(A(t)) \quad (8)$$

Moreover, (8) implies that the values of the approximated function and the original function at the interpolation points are identical. i.e.

$$M(\hat{A}(t)) = M(\mathcal{U}c(t)) = M(A(t))$$

Here $M\mathcal{U}$ is a linear operator. Assuming $M\mathcal{U}$ as an invertible operator, we have

$$c(t) = (M\mathcal{U})^{-1} M(A(t))$$

This means

$$\hat{A}(t) = \mathcal{U}c(t) = \mathcal{U}(M\mathcal{U})^{-1} M(A(t)) \quad (9)$$

Now, there are three challenges to deal with. Firstly, we have to define the operator \mathcal{U} so that it is computationally efficient. However, all masking operators cannot guarantee the existence of the inverse of the operator $M\mathcal{U}$ (see (9)). Therefore, we define a masking operator to ensure the existence of the inverse of the operator $M\mathcal{U}$, which is our second challenge. Finally, the third challenge is to select the appropriate representation for M , that will yield computationally efficient approximations of matrix-valued functions $A(t)$. In Section 2.2, we comprehensively examine the first challenge. Subsequently, in Section 3, we address the second challenge by presenting a detailed analysis of the utilized representation of M , revealing its computationally inefficient form (15). The subsequent segments of the paper are dedicated to the derivation of an appropriate representation for M . This new representation is engineered to be computationally more efficient compared to the previously employed version (refer Table 3).

2.1 POD Using Tensor

In this section, we introduce a method for deriving the global basis function (tensor Proper Orthogonal Decomposition (POD) basis) of the matrix $A(t)$. This POD basis serves as the foundation for defining the operator \mathcal{U} , which offers enhanced computational efficiency during the offline stage when compared to the Matrix Discrete Empirical Interpolation Method (MDEIM) [19]. Notably, \mathcal{U} operates directly on the matrix without requiring vectorization.

To construct our POD basis, we employ a tensor-based approach. This tensor basis may not guarantee the optimal k-rank approximation (for more details, refer to section 3.2 of [42]); however, it is particularly advantageous for handling large matrices due to its computational efficiency [50].

Furthermore, we have standardized the data by centering it around zero mean. This normalization enhances the ability to capture variations in the data robustly.

A tensor is a multi-linear functional. More specifically, a functional $T: \mathbb{R}^{L_1} \times \mathbb{R}^{L_2} \times \dots \times \mathbb{R}^{L_p} \rightarrow \mathbb{R}$ of order-p defined on a Cartesian product of Hilbert spaces \mathbb{R}^{L_k} (for detail refer [32, 42, 31]). For the given tensor $T: \mathbb{R}^{L_1} \times \mathbb{R}^{L_2} \times \mathbb{R}^{L_3} \rightarrow \mathbb{R}$, a *modal-rank decomposition* is given as

$$T = \sum_{l_1=1}^{L_1} \sum_{l_2=1}^{L_2} \sum_{l_3=1}^{L_3} \sigma_{l_1 l_2 l_3} u_1^{(l_1)} \otimes u_2^{(l_2)} \otimes u_3^{(l_3)} \quad (10)$$

where the vectors in the set $\{u_i^{(l_i)}\}_{1 \leq l_i \leq R_i}$ are mutually orthonormal for each $i \in \{1, 2, 3\}$. The vector (L_1, L_2, L_3) is known as the *modal rank* of the given tensor (for details, refer [32]). An approximation of a tensor can be obtained by truncation of the summation in (10) up to α_i instead of L_i for $i \in \{1, 2, 3\}$. Here, we use higher-order singular value Decomposition (HOSVD) as given in [32].

For our case, we assume that $T = (A(t_1), A(t_2), \dots, A(t_N))$, where $A(t_i) \in \mathbb{R}^{n_1 \times n_2}$ is value of matrix-valued function at time-step $t_i \in \mathbb{R}$. Therefore, T is an order-3 tensor, with time being the third dimension. In this work, we have not considered the truncation in time direction as it most common way in model reduction but few techniques exist in literature like [44] which considers the truncation in time direction also. Using the above-mentioned methods, a (m_1, m_2, N) - modal rank approximation of the tensor T is given as

$$T = \sum_{l_1=1}^{m_1} \sum_{l_2=1}^{m_2} \sum_{l_3=1}^N \sigma_{l_1 l_2 l_3} u_1^{(l_1)} \otimes u_2^{(l_2)} \otimes u_3^{(l_3)}$$

where each $u_1^{(i)} \in \mathbb{R}^{n_1}$, $u_2^{(i)} \in \mathbb{R}^{n_2}$ and $u_3^{(i)} \in \mathbb{R}^N$.

Thus, we can define operator \mathcal{U} as,

$$\mathcal{U}x = \sum_{i=1}^{m_1} \sum_{j=1}^{m_2} \langle x, e_1^{(i)} \otimes e_2^{(j)} \rangle u_1^{(i)} \otimes u_2^{(j)} \quad (11)$$

In case of matrices, it is guaranteed that the optimal k-rank approximation can be achieved using Singular Value Decomposition (SVD), ensuring optimality. However, this statement does not hold true when dealing with tensors [42]. As a result, the subspace represented by $m_1 m_2$ bases in (11) may not necessarily be optimal.

An alternate approach to compute the basis is by using the matrix flattening approach as described in [19]. Assume that columns of a matrix $U_f \in \mathbb{R}^{n_1 n_2 \times k}$ represent the POD basis of $\text{vec}(A(t))$. This U_f can be approximated as a Kronecker product of two matrices as in [33].

$$U_f \approx U_1 \otimes_k U_2$$

2.2 Computationally Efficient form of \mathcal{U}

The advantage of using (11) is that \mathcal{U} can be written in a matrix product form, which is computationally efficient. Thus, we propose the following lemma.

Lemma 1. Let $T: \mathbb{R}^{m_1 \times m_2} \rightarrow \mathbb{R}^{n_1 \times n_2}$ be an operator given by

$$TX = \sum_{i=1}^{m_1} \sum_{j=1}^{m_2} \langle X, v_1^{(i)} \otimes v_2^{(j)} \rangle u_1^{(i)} \otimes u_2^{(j)}$$

then

$$TX = U_1 V_2 X V_1^T U_2^T$$

where $U_k = \begin{bmatrix} u_k^{(1)} & u_k^{(2)} & \dots & u_k^{(r_k)} \end{bmatrix}$ and $V_k = \begin{bmatrix} v_k^{(1)} & v_k^{(2)} & \dots & v_k^{(r_k)} \end{bmatrix}$ for $k \in \{1, 2\}$.

Proof. Given that

$$\sum_{i=1}^{m_1} \sum_{j=1}^{m_2} b_{ij} u_1^{(i)} \otimes u_2^{(j)} = U_1 B U_2^T$$

where $B \in \mathbb{R}^{m_1 \times m_2}$. Also,

$$b_{ij} = \langle X, v_1^{(i)} \otimes v_2^{(j)} \rangle = \text{tr}(X v_1^{(i)} (v_2^{(j)})^T) = (v_2^{(j)})^T X v_1^{(i)}$$

Above expression of $b_{ij} = (v_2^{(j)})^T X v_1^{(i)}$ implies that $B = V_2 X V_1^T$. Now, the result follows. \square

Using the result of lemma 1, the following result can be obtained,

Corollary 1. Let \mathcal{U} be as in (11). Then,

$$\mathcal{U}X = U_1 X U_2^T \quad (12)$$

where $U_k = \begin{bmatrix} u_1^{(k)} & u_2^{(k)} & \dots & u_{m_k}^{(k)} \end{bmatrix}$.

2.3 Inverse of the operator $M\mathcal{U}$

As discussed in Section 2, matrix approximation can be obtained using (9); a masking operator M and $(MU)^{-1}$ is needed for this purpose. This section mainly emphasizes defining $(MU)^{-1}$ operator. Applying masking operator M on (11) results in

$$M(\mathcal{U}X) = \sum_{i=1}^{m_1} \sum_{j=1}^{m_2} \langle x, e_1^{(i)} \otimes e_2^{(j)} \rangle M(u_1^{(i)} \otimes u_2^{(j)})$$

Although $u_1^{(i)} \otimes u_2^{(j)}$ is a rank-1 operator, $M(u_1^{(i)} \otimes u_2^{(j)})$ may not result in rank-1 operator. As a result of this, the masking operator M needs to be selected such that $(MU)^{-1}$ exists. The EIM algorithm helps us in this regard (refer to Section 2 of [14]). The rest of the discussion in this section is centered around calculating $(MU)^{-1}$.

Lemma 2. Let M and \mathcal{U} be defined as in (6) and (11). Then

$$\text{vec}(M(\mathcal{U}X)) = ((P_2 U_2)^T \otimes_{kr} (P_1 U_1)^T)^T \text{vec}(X) \quad (13)$$

where

$$P_1^T = \begin{bmatrix} e_{i_1} & e_{i_2} & \dots & e_{i_{m_1 m_2}} \end{bmatrix}$$

$$P_2^T = \begin{bmatrix} e_{j_1} & e_{j_2} & \dots & e_{j_{m_1 m_2}} \end{bmatrix}$$

where, $e_k \in \mathbb{R}^n$ is the standard unit vector.

Proof. Since $\mathcal{U}X = U_1 X U_2^T$, we have that

$$\text{vec}(\mathcal{U}X) = (U_2 \otimes_k U_1) \text{vec}(X)$$

The rest of the proof follows from (7) and the definition of the Khatri-rao product (refer, e.g., [42]). \square

Lemma 3. Let M and \mathcal{U} be as in (6) and (11). If $(MU)^{-1}$ exist, then

$$\text{vec}((MU)^{-1} X) = (((P_2 U_2)^T \otimes_{kr} (P_1 U_1)^T)^T)^{-1} \text{vec}(X)$$

Proof. Let, $M_u = (((P_2 U_2)^T \otimes_{kr} (P_1 U_1)^T)^T)^{-1}$. For a given matrix X of appropriate dimension, using Lemma 2, we have

$$\text{vec}(X) = \text{vec}((MU)(MU)^{-1} X) = M_u \text{vec}((MU)^{-1} X)$$

Hence, the result. \square

3 Tensor Empirical Interpolation Method (TEIM)

This section explains the method for obtaining the mask operator M (see (9)) and approximating the matrix-valued function from it. This method is referred as *tensor empirical interpolation method (TEIM)* in the subsequent discussions. The masking operator can be obtained by applying the DEIM method, but it requires the tensor basis $u_i \otimes u_j$ to be transferred into equivalent vector form using the *vec* operator. However, in order to achieve a memory-efficient implementation without disrupting the tensor product structure, we have updated the EIM algorithm. In this algorithm (TEIM), a nested set of interpolation points are selected such that for all $1 \leq m_1 \leq n_1$ and $1 \leq m_2 \leq n_2$, $(MU)^{-1}$ exists.

noresize (TEIM) To obtain the mask function. r_{ij} denotes the (i, j) element of matrix R .

```

Input  $U = [u_1 \ u_2 \ \dots \ u_{m_1}]$ ,  $V = [v_1 \ v_2 \ \dots \ v_{m_2}]$ ,  $P_1 = 0$  and  $P_2 = 0$ 
Output  $P_1$  and  $P_2$ 
for  $k = 1, \dots, m_1$  do
  for  $l = 1, \dots, m_2$  do
    if  $k = 1$  and  $l = 1$  then
       $[\phi_1^1, \phi_1^2] = \text{argmax}_{i,j} u_1 v_1^T$ 
       $P_1 = [e_{\phi_1^1}]$ ,  $P_2 = [e_{\phi_1^2}]$ 
       $U_1 = [u_1]$ ,  $U_2 = [v_1]$ 
    else
       $c = \text{inv}((P_1^T U_1) \cdot (P_2^T U_2))((P_1^T u_k) \cdot (P_2^T v_l))$ 
       $R = u_k v_l^T - \sum_{i=1}^{k-1} \sum_{j=1}^{m_2} c((i-1)m_2 + j) * u_i v_j^T - \sum_{j=1}^{l-1} c((k-1)m_2 + j) * u_k v_j^T$ 
       $(p_{k1}, p_{k2}) = \text{argmax}_{i,j} |r_{ij}|$ 
       $P_1 = [P_1 \ e_{p_{k1}}]$ 
       $P_2 = [P_2 \ e_{p_{k2}}]$ 
       $U_1 = [U_1 \ u_k]$ 
       $U_2 = [U_2 \ v_l]$ 
    end if
  end for
end for
return  $P_1, P_2$ 

```

Using (9), the approximated $\tilde{A}(x)$ can be written as

$$\tilde{A}(t) = \mathcal{U}((MU)^{-1}M(A(t)))$$

Where $\mathcal{U}X = U_1 X U_2^T$. Therefore

$$\tilde{A}(t) = U_1((MU)^{-1}M(A(t)))U_2^T \quad (14)$$

The (14) can be written in vectorized form as

$$\text{vec}(\tilde{A}(t)) = (U_2 \otimes_k U_1) \text{vec}((MU)^{-1}M(A(t)))$$

Using the result of Lemma 2 and 3

$$\text{vec}(\tilde{A}(t)) = (U_2 \otimes_k U_1)((P_2 U_2)^T \otimes_{kr} (P_1 U_1)^T)^{-1} \text{vec}(M(A(t))) \quad (15)$$

The current representation of masking operator M represented in terms of P_1 and P_2 ($MX = \text{vec}^{-1}[(P_2^T \otimes_{kr} P_1^T) \text{vec}(X)]$) has the following disadvantages.

- The expression for the approximation of $A(t)$ as presented in (15) illustrates that despite $A(t)$ being a matrix-valued function, the approximation procedure requires it to be represented in equivalent vector form $\text{vec}(M(A(t)))$. Thus, the resulting process becomes akin to approximating vector-valued functions. This outcome doesn't align with our objective, as our motive is to approximate the matrix-valued function without transforming it into a vectorized form.
- Additionally, the online computational needed to approximate the equivalent representation, $\text{vec}(A(t))$, amounts to $n^2 m_1 m_2$ using (15). This stems from the fact that the matrix $(U_2 \otimes_k U_1)((P_2 U_2)^T \otimes_{kr} (P_1 U_1)^T)^{-1}$ has dimensions of $n^2 \times m_1 m_2$ and can be precomputed offline.

3.1 Computationally Efficient Form of MU

In the preceding section, we constructed a masking operator using the TEIM algorithm and employed it for approximating $A(t)$. However, the approximation process bears a resemblance to approximating a vector-valued function. In this section, we've deduced an alternate form of the masking operator M . Besides being computationally efficient, this improved representation of M also assists our objective of approximating the matrix-valued function without transforming it into a vectorized form.

Lemma 4. Let $a \in \mathbb{R}^{m_1}$, $b \in \mathbb{R}^{m_2}$, and i, j denote the index corresponding to the maximum element of $|a|$ and $|b|$ respectively then the index of maximum element of matrix $|ab^T|$ will be at (i, j) .

Lemma 4 is consequential in deriving a new representation for the masking operator and exploring the structure present in P_1 and P_2 , which is explored in theorem 1 as given below.

Theorem 1. Let $P_1 \in \mathbb{R}^{m_1 m_2 \times n_1}$ and $P_2 \in \mathbb{R}^{m_1 m_2 \times n_2}$ are obtained from TEIM algorithm then there exist $P_3 \in \mathbb{R}^{m_1 \times n_1}$ and $P_4 \in \mathbb{R}^{m_2 \times n_2}$ such that

$$P_1^T \otimes_{kr} P_2^T = P_3^T \otimes_k P_4^T$$

and $P_3^T(:, i) = P_1^T(:, i * m_2 + 1)$, $P_4^T(:, j) = P_2^T(:, j)$. where $i \in \{1, 2, \dots, m_1\}$ and $j \in \{1, 2, \dots, m_2\}$.

Proof. Let us assume the following definitions for iteration sets, representing the collection of iterations associated with distinct values of the outer "for" loop (varying values of k) within the algorithm (TEIM).

$$\begin{aligned} s_1 &= \{1, 2, 3, \dots, m_2\} \\ s_2 &= \{m_2 + 1, m_2 + 2, m_2 + 3, \dots, 2m_2\} \\ &\vdots \\ s_{m_1} &= \{(m_1 - 1)m_2 + 1, (m_1 - 1)m_2 + 2, \dots, m_1 m_2\} \end{aligned}$$

This proof establishes that the interpolation points selected by the TEIM algorithm forms a rectangular grid, which has been shown using the concept of *mathematical induction*. We show that, for each iteration within a specified iteration set, the algorithm selects interpolation points such that they share the same row but occupy different columns. Furthermore, the columns chosen for one iteration set remain consistent across all other iteration sets. Notation $\mathbf{v}_{(i,j)}$ and $\mathbf{c}_{(\ell,j)}$ are used to represent j^{th} element of vector \mathbf{v}_i and coefficients vector \mathbf{c}_ℓ of iteration ℓ , respectively.

For any arbitrary iteration l of iteration set s_1 (for $n = 1$ in terms of induction), the residual is of the following form

$$\begin{aligned} R_\ell &= \mathbf{u}_1 \otimes_k \mathbf{v}_\ell^T - \sum_{i=1}^{\ell-1} \mathbf{c}_{(\ell,i)} (\mathbf{u}_1 \otimes_k \mathbf{v}_i^T) \\ &= \mathbf{u}_1 \otimes_k \left(\mathbf{v}_\ell - \sum_{i=1}^{\ell-1} \mathbf{c}_{(\ell,i)} \mathbf{v}_i \right)^T \end{aligned}$$

This residual is a rank one matrix involving the vectors \mathbf{u}_1 and $\mathbf{v}_\ell - \sum_{i=1}^{\ell-1} \mathbf{c}_{(\ell,i)} \mathbf{v}_i$ where the coefficients vector \mathbf{c}_ℓ can be computed from the set of linear equations as shown below.

$$\begin{bmatrix} \mathbf{v}_{(1,j_1)} & \mathbf{v}_{(2,j_1)} & \dots & \mathbf{v}_{(\ell-1,j_1)} \\ \mathbf{v}_{(1,j_2)} & \mathbf{v}_{(2,j_2)} & \dots & \mathbf{v}_{(\ell-1,j_2)} \\ \vdots & \vdots & \dots & \vdots \\ \mathbf{v}_{(1,j_{\ell-1})} & \mathbf{v}_{(2,j_{\ell-1})} & \dots & \mathbf{v}_{(\ell-1,j_{\ell-1})} \end{bmatrix} \begin{bmatrix} \mathbf{c}_{(\ell,1)} \\ \mathbf{c}_{(\ell,2)} \\ \vdots \\ \mathbf{c}_{(\ell,\ell-1)} \end{bmatrix} = \begin{bmatrix} \mathbf{v}_{(\ell,j_1)} \\ \mathbf{v}_{(\ell,j_2)} \\ \vdots \\ \mathbf{v}_{(\ell,j_{\ell-1})} \end{bmatrix} \quad (16)$$

Table 1 reveals that the left vector of residual for every iteration within the set s_1 is identical to \mathbf{u}_1 . Consequently, employing Lemma 4, if i_1 represents the index of the maximum element of $|\mathbf{u}_1|$, it follows that the maximum element of the residual for each iteration within the iteration set s_1 will also correspond to the same (i_1^{th}) row. Suppose the index of the maximum element of vector $|\mathbf{v}_\ell - \sum_{i=1}^{\ell-1} \mathbf{c}_{(\ell,i)} \mathbf{v}_i|$ is j_ℓ then columns selected by algorithm (TEIM) are $(j_1, j_2, \dots, j_{m_2})$ for iteration set s_1 .

Let a rectangular grid structure of interpolation points extend up to the iteration set s_{k-1} . Here, the term s_{k-1} denotes the stage up to the iteration $(k-1)m_2$, where $k-1$ rows have been chosen denoted by $(i_1, i_2, \dots, i_{k-1})$. An identical set of m_2 columns is also chosen from each of these selected rows, with their indices represented as $(j_1, j_2, \dots, j_{m_2})$.

Iteration Number	Residual Matrix	Left Vector	Right Vector
1	$\mathbf{u}_1 \mathbf{v}_1^T$	\mathbf{u}_1	\mathbf{v}_1
2	$\mathbf{u}_1 (\mathbf{v}_2 - \mathbf{c}_{(2,1)} \mathbf{v}_1)^T$	\mathbf{u}_1	$\mathbf{v}_2 - \mathbf{c}_{(2,1)} \mathbf{v}_1$
3	$\mathbf{u}_1 (\mathbf{v}_3 - \mathbf{c}_{(3,1)} \mathbf{v}_1 - \mathbf{c}_{(3,2)} \mathbf{v}_2)^T$	\mathbf{u}_1	$\mathbf{v}_3 - \mathbf{c}_{(3,1)} \mathbf{v}_1 - \mathbf{c}_{(3,2)} \mathbf{v}_2$
.	.	.	.
.	.	.	.
j	$\mathbf{u}_1 (\mathbf{v}_j - \sum_{i=1}^{j-1} \mathbf{c}_{(j,i)} \mathbf{v}_i)^T$	\mathbf{u}_1	$\mathbf{v}_j - \sum_{i=1}^{j-1} \mathbf{c}_{(j,i)} \mathbf{v}_i$
.	.	.	.
.	.	.	.
m_2	$\mathbf{u}_1 (\mathbf{v}_{m_2} - \sum_{i=1}^{m_2-1} \mathbf{c}_{(m_2,i)} \mathbf{v}_i)^T$	\mathbf{u}_1	$\mathbf{v}_{m_2} - \sum_{i=1}^{m_2-1} \mathbf{c}_{(m_2,i)} \mathbf{v}_i$

Table 1: Residual matrix for the iterations of Iteration set s_1

For any arbitrary element ℓ of a given iteration set s_k corresponding to iteration number $(k-1)m_2 + \ell$, residual is of the below form

$$R_{(k-1)m_2+\ell} = \mathbf{u}_k \mathbf{v}_\ell^T - \sum_{i=1}^{k-1} \sum_{j=1}^{m_2} \mathbf{c}_{((k-1)m_2+\ell), (i-1)m_2+j} \mathbf{u}_i \mathbf{v}_j^T - \sum_{i=1}^{\ell-1} \mathbf{c}_{((k-1)m_2+\ell), (k-1)m_2+i} \mathbf{u}_k \mathbf{v}_i^T$$

Suppose $\mathbf{G}, \mathbf{H}, \mathbf{w}, \mathbf{q}, \mathbf{r}$ and \mathbf{z} are defined as below

$$\mathbf{r} = \begin{bmatrix} \mathbf{u}_{(1,i_k)} \\ \mathbf{u}_{(2,i_k)} \\ \vdots \\ \mathbf{u}_{(k-1,i_k)} \end{bmatrix}, \mathbf{z} = \begin{bmatrix} \mathbf{v}_{(1,j_1)} \\ \mathbf{v}_{(1,j_2)} \\ \vdots \\ \mathbf{v}_{(1,j_{m_2})} \end{bmatrix}$$

$$\mathbf{G} = \begin{bmatrix} \mathbf{u}_{(1,i_1)} & \mathbf{u}_{(2,i_1)} & \cdots & \mathbf{u}_{(k-1,i_1)} \\ \mathbf{u}_{(1,i_2)} & \mathbf{u}_{(2,i_2)} & \cdots & \mathbf{u}_{(k-1,i_2)} \\ \vdots & \vdots & \cdots & \vdots \\ \mathbf{u}_{(1,i_{k-1})} & \mathbf{u}_{(2,i_{k-1})} & \cdots & \mathbf{u}_{(k-1,i_{k-1})} \end{bmatrix}$$

$$\mathbf{H} = \begin{bmatrix} \mathbf{v}_{(1,j_1)} & \mathbf{v}_{(2,j_1)} & \cdots & \mathbf{v}_{(k-1,j_1)} \\ \mathbf{v}_{(1,j_2)} & \mathbf{v}_{(2,j_2)} & \cdots & \mathbf{v}_{(k-1,j_2)} \\ \vdots & \vdots & \cdots & \vdots \\ \mathbf{v}_{(1,j_{m_2})} & \mathbf{v}_{(2,j_{m_2})} & \cdots & \mathbf{v}_{(k-1,j_{m_2})} \end{bmatrix}$$

$$\mathbf{w} = \begin{bmatrix} \mathbf{u}_{(k,i_1)} \\ \mathbf{u}_{(k,i_2)} \\ \vdots \\ \mathbf{u}_{(k,i_{k-1})} \end{bmatrix}, \mathbf{q} = \begin{bmatrix} \mathbf{v}_{(k,j_1)} \\ \mathbf{v}_{(k,j_2)} \\ \vdots \\ \mathbf{v}_{(k,j_{m_2})} \end{bmatrix}$$

Then, the system of linear equation for evaluating the coefficient vector $\mathbf{c}_{((k-1)m_2+\ell)}$ is given as

$$\begin{bmatrix} \mathbf{G} \otimes_k \mathbf{H} & \mathbf{w} \otimes_k \mathbf{H}(:, 1 : \ell - 1) \\ \mathbf{r}^T \otimes_k \mathbf{H}(1 : \ell - 1, :) & \mathbf{u}_{k,i_k} \otimes_k \mathbf{H}(1 : \ell - 1, 1 : \ell - 1) \end{bmatrix} \begin{bmatrix} \mathbf{x} \\ \mathbf{y} \end{bmatrix} = \begin{bmatrix} \mathbf{b}_1 \\ \mathbf{b}_2 \end{bmatrix} \quad (17)$$

Here, $\mathbf{b}_1 = \mathbf{w} \otimes_k \mathbf{z}$, $\mathbf{b}_2 = \mathbf{u}_{(k,i_k)} \otimes_k \mathbf{z}(1 : \ell - 1)$, \mathbf{x} and \mathbf{y} encompass all the coefficients associated with the second term and third term of the residual $R_{(k-1)m_2+\ell}$ respectively. Owing to the fact that TEIM is an extension of empirical interpolation method [14], invertibility of $(\mathbf{G} \otimes_k \mathbf{H})$ is assured. As a result, equation (17) can be solved using Schur

complement [36]. Using this \mathbf{y} can be expressed as

$$\begin{aligned}
\mathbf{y} &= (\mathbf{u}_{(\mathbf{k}, i_k)} \otimes_k \mathbf{H}(1 : \ell - 1, 1 : \ell - 1) - \mathbf{r}^T \otimes_k \mathbf{H}(1 : \ell - 1, :))(\mathbf{G}^{-1} \otimes_k \mathbf{H}^{-1}) \\
&\quad * (\mathbf{w} \otimes_k \mathbf{H}(:, 1 : \ell - 1))^{-1} \mathbf{u}_{(\mathbf{k}, i_k)} \otimes_k \mathbf{z}(1 : \ell - 1) - \mathbf{r}^T \otimes_k \mathbf{H}(1 : \ell - 1, :) \\
&\quad * (\mathbf{G}^{-1} \otimes_k \mathbf{H}^{-1})(\mathbf{w} \otimes_k \mathbf{z}) \\
&= (\mathbf{u}_{(\mathbf{k}, i_k)} \otimes_k \mathbf{H}(1 : \ell - 1, 1 : \ell - 1) - \mathbf{r}^T \mathbf{G}^{-1} \mathbf{w} \otimes_k \mathbf{H}(1 : \ell - 1, :)) \mathbf{H}^{-1} \\
&\quad * \mathbf{H}(:, 1 : \ell - 1))^{-1} \mathbf{u}_{(\mathbf{k}, i_k)} \otimes_k \mathbf{z}(1 : \ell - 1) - \mathbf{r}^T \mathbf{G}^{-1} \mathbf{w} \otimes_k \mathbf{H}(1 : \ell - 1, :)) \mathbf{H}^{-1} \mathbf{z}
\end{aligned}$$

Suppose P_h is an operator which select $\ell - 1$ rows of \mathbf{H} as defined below

$$P_h \mathbf{H} = \mathbf{H}(1 : \ell - 1, :)$$

Then, $\mathbf{H}(1 : \ell - 1, :)\mathbf{H}^{-1}\mathbf{H}(:, 1 : \ell - 1))^{-1} = P_h \mathbf{H} \mathbf{H}^{-1} \mathbf{H}(:, 1 : \ell - 1) = P_h \mathbf{H}(:, 1 : \ell - 1) = \mathbf{H}(1 : \ell - 1, 1 : \ell - 1)$ and similarly $\mathbf{H}(1 : \ell - 1, :)\mathbf{H}^{-1}\mathbf{z} = \mathbf{z}(1 : \ell - 1)$. Using this, \mathbf{y} can be further reduced as below

$$\begin{aligned}
\mathbf{y} &= (\mathbf{u}_{(\mathbf{k}, i_k)} - \mathbf{r}^T \mathbf{G}^{-1} \mathbf{w})^{-1} \mathbf{H}(1 : \ell - 1, 1 : \ell - 1)^{-1} \\
&\quad * (\mathbf{u}_{(\mathbf{k}, i_k)} - \mathbf{r}^T \mathbf{G}^{-1} \mathbf{w}) \mathbf{z}(1 : \ell - 1) \\
&= \mathbf{H}(1 : \ell - 1, 1 : \ell - 1)^{-1} \mathbf{z}(1 : \ell - 1) \\
&= \begin{bmatrix} \mathbf{v}_{(1, j_1)} & \mathbf{v}_{(2, j_1)} & \cdots & \mathbf{v}_{(\ell-1, j_1)} \\ \mathbf{v}_{(1, j_2)} & \mathbf{v}_{(2, j_2)} & \cdots & \mathbf{v}_{(\ell-1, j_2)} \\ \vdots & \vdots & \cdots & \vdots \\ \mathbf{v}_{(1, j_{\ell-1})} & \mathbf{v}_{(2, j_{\ell-1})} & \cdots & \mathbf{v}_{(\ell-1, j_{\ell-1})} \end{bmatrix}^{-1} \begin{bmatrix} \mathbf{v}_{(\ell, j_1)} \\ \mathbf{v}_{(\ell, j_2)} \\ \vdots \\ \mathbf{v}_{(\ell, j_{\ell-1})} \end{bmatrix} \tag{18}
\end{aligned}$$

Equation (18) and (16) imply that coefficients involved in residual corresponding to iteration ℓ and y are the same. Similarly, \mathbf{x} can be evaluated using Schur's complement as follows

$$x = (\mathbf{G}^{-1} \otimes_k \mathbf{H}^{-1}) \mathbf{w} \otimes_k \mathbf{z} - (\mathbf{G}^{-1} \otimes_k \mathbf{H}^{-1}) \mathbf{w} \otimes_k \mathbf{H}(:, 1 : \ell - 1) \mathbf{y} \tag{19}$$

$$= (\mathbf{G}^{-1} \mathbf{w} \otimes_k \mathbf{H}^{-1} \mathbf{z}) - (\mathbf{G}^{-1} \mathbf{w} \otimes_k \mathbf{H}^{-1} \mathbf{H}(:, 1 : \ell - 1) \mathbf{y}) \tag{20}$$

$$= (\mathbf{G}^{-1} \mathbf{w}) \otimes_k (\mathbf{H}^{-1} \mathbf{z} - \mathbf{H}^{-1} \mathbf{H}(:, 1 : \ell - 1) \mathbf{y}) \tag{21}$$

$$= (\mathbf{G}^{-1} \mathbf{w}) \otimes_k \left(\begin{bmatrix} 0 \\ 0 \\ \vdots \\ 0 \\ 1 \\ 0 \\ \vdots \\ 0 \end{bmatrix} - \begin{bmatrix} \mathbf{y}_1 \\ \mathbf{y}_2 \\ \vdots \\ \mathbf{y}_{\ell-1} \\ 0 \\ 0 \\ \vdots \\ 0 \end{bmatrix} \right) = (\mathbf{G}^{-1} \mathbf{w} \otimes_k \begin{bmatrix} \mathbf{y}_1 \\ \mathbf{y}_2 \\ \vdots \\ \mathbf{y}_{\ell-1} \\ 1 \\ 0 \\ \vdots \\ 0 \end{bmatrix}) \tag{22}$$

Using (18) and (22), residual corresponding to iteration $(k-1)m_2 + \ell$ can be reduced as follows

$$\begin{aligned}
R_{(k-1)m_2+\ell} &= \mathbf{u}_k \mathbf{v}_\ell^T - \sum_{i=1}^{k-1} \sum_{j=1}^{\ell} \mathbf{c}_{((k-1)m_2+\ell), (i-1)m_2+j} \mathbf{u}_i \mathbf{v}_j^T \\
&\quad - \sum_{i=1}^{\ell-1} \mathbf{c}_{((k-1)m_2+\ell), (k-1)m_2+i} \mathbf{u}_k \mathbf{v}_i^T \\
&= \mathbf{u}_k (\mathbf{v}_\ell^T - \sum_{i=1}^{\ell-1} \mathbf{c}_{((k-1)m_2+\ell), (k-1)m_2+i} \mathbf{v}_i^T) \\
&\quad - \sum_{j=1}^{k-1} \sum_{i=1}^{\ell-1} (\mathbf{G}^{-1} \mathbf{w})_j \mathbf{u}_j^* \\
&\quad \quad (\mathbf{v}_\ell^T - \mathbf{c}_{((k-1)m_2+\ell), (k-1)m_2+i} \mathbf{v}_i^T) \\
&= (\mathbf{u}_k - \sum_{j=1}^{k-1} (\mathbf{G}^{-1} \mathbf{w})_j \mathbf{u}_j) \\
&\quad * (\mathbf{v}_\ell^T - \sum_{i=1}^{\ell-1} \mathbf{c}_{((k-1)m_2+\ell), (k-1)m_2+i} \mathbf{v}_i^T)
\end{aligned}$$

As $\mathbf{c}_{((k-1)m_2+\ell), (k-1)m_2+i} = \mathbf{c}_{(\ell, i)}$ and $\mathbf{c}_{((k-1)m_2+\ell), (j-1)m_2+1} = (\mathbf{G}^{-1} \mathbf{w})_j$ then, residual can be further simplified as below

$$\begin{aligned}
R_{(k-1)m_2+l} &= (\mathbf{u}_k - \sum_{j=1}^{k-1} \mathbf{c}_{((j-1)m_2+\ell), (k-1)m_2+1} \mathbf{u}_j) \\
&\quad * (\mathbf{v}_\ell^T - \sum_{i=1}^{\ell-1} \mathbf{c}_{(\ell, i)} \mathbf{v}_i^T)
\end{aligned} \tag{23}$$

Iteration No.	Residual Matrix	Left Vector	Right Vector
$(k-1)m_2 + 1$	$(u_k - \sum_{j=1}^{k-1} c_{(j-1)m_2+1}^{(k-1)m_2+1} u_j) v_1^T$	$u_k - \sum_{j=1}^{k-1} c_{(j-1)m_2+1}^{(k-1)m_2+1} u_j$	v_1
$(k-1)m_2 + 2$	$(u_k - \sum_{j=1}^{k-1} (c_{(j-1)m_2+1}^{(k-1)m_2+1} u_j) (v_2 - c_1^2 v_1)$	$(u_k - \sum_{j=1}^{k-1} (c_{(j-1)m_2+1}^{(k-1)m_2+1} u_j)$	$v_2 - c_1^2 v_1$
.	.	.	.
.	.	.	.
$(k-1)m_2 + l$	$(u_k - \sum_{j=1}^{k-1} (c_{(j-1)m_2+1}^{(k-1)m_2+1} u_j) (v_l^T - \sum_{i=1}^{l-1} c_i^l u_k v_i^T)$	$(u_k - \sum_{j=1}^{k-1} (c_{(j-1)m_2+1}^{(k-1)m_2+1} u_j)$	$v_l - \sum_{i=1}^{j-1} c_i v_i$
.	.	.	.
.	.	.	.
km_2	$(u_k - \sum_{j=1}^{k-1} (c_{(j-1)m_2+1}^{(k-1)m_2+1} u_j) (v_{m_2} - \sum_{i=1}^{m_2-1} c_i v_i)^T$	$(u_k - \sum_{j=1}^{k-1} (c_{(j-1)m_2+1}^{(k-1)m_2+1} u_j)$	$v_{m_2} - \sum_{i=1}^{m_2-1} c_i v_i$

Table 2: Residual Matrix Table for Iteration set s_k

Equation (23) demonstrates that across all iterations within iteration set s_k , the interpolation points follows a pattern where all these points are confined within a single row, while the columns align with the previously selected columns $(j_1, j_2, \dots, j_{m_2})$ in other iteration sets. This observation is evident from Tables 2 and 1.

Suppose the below iteration set is defined for constructing P_2

$$\begin{aligned}
t_1 &= \{1, m_2 + 1, 2m_2 + 1, \dots, (m_1 - 1)m_2 + 1\} \\
t_2 &= \{2, m_2 + 2, 2m_2 + 2, \dots, (m_1 - 1)m_2 + 2\} \\
&\vdots \\
t_{m_2} &= \{m_2, 2m_2, 3m_2, \dots, (m_1 - 1)m_2 + m_2\}
\end{aligned}$$

Based on Tables 1 and 2, it is evident that for iterations within the s_k iteration set, an identical vector is consistently appended to P_1^T . Similarly, in the case of iterations within the t_k iteration set, an identical vector is appended to

P_2^T . Using P_1 and P_2 , if we construct P_3 and P_4 as $P_3^T(:, i) = P_1^T(:, i \cdot m_2 + 1)$ and $P_4^T(:, j) = P_2^T(:, j)$, where $i \in \{1, 2, \dots, m_1\}$ and $j \in \{1, 2, \dots, m_2\}$, then from the definition of Kronecker and column-wise Khatri-Rao product, ...

$$P_1^T \otimes_{kr} P_2^T = P_3^T \otimes_k P_4^T$$

□

Similar to the TEIM algorithm, the discrete empirical interpolation method [15] is also an extension of the empirical interpolation method [14]. The connection between the new masking operator (P_3, P_4) and the DEIM masking operator (P_5, P_6) obtained from Algorithm 2 is established in Theorem 2.

noresize 2 2D-DEIM. See [15] or appendix for DEIM algorithm

Input $U = [u_1 \ u_2 \ \dots \ u_{m_1}]$, $V = [v_1 \ v_2 \ \dots \ v_{m_2}]$, $P_5 = 0$ and $P_6 = 0$

Output P_5 and P_6

$[P_5, \Phi_1] = DEIM(U)$

$[P_6, \Phi_2] = DEIM(V)$

return P_5, P_6

The 2D-DEIM algorithm allows for the direct derivation of masking operators P_3 and P_4 , eliminating the need for the TEIM algorithm, which was employed in [38] without any accompanying mathematical justification.

Theorem 2. Suppose P_5 and P_6 are the masking operators obtained by applying the Discrete Empirical Interpolation Algorithm on columns of U_1 and U_2 , respectively. Then $P_3 = P_5$ and $P_4 = P_6$.

Proof. As per equation (23), the residual conforms to the following structure for any given iteration set s_k . Within this iteration set s_k , the same structure holds true for any arbitrary element l .

$$\begin{aligned} \max(|R_{(k-1)m_2+l}|) &= \max(|\mathbf{u}_k - \sum_{j=1}^{k-1} \mathbf{c}_{((j-1)m_2+\ell, (k-1)m_2+1)} \mathbf{u}_j|) \\ &\quad * \max(|\mathbf{v}_\ell^T - \sum_{i=1}^{\ell-1} \mathbf{c}_{(\ell, i)} \mathbf{v}_i^T|) \\ &= \max(r_1) \max(r_2) \end{aligned}$$

$$\text{Where } r_1 = \mathbf{u}_k - \sum_{j=1}^{k-1} \mathbf{c}_{((j-1)m_2+\ell, (k-1)m_2+1)} \mathbf{u}_j \text{ and } r_2 = \mathbf{v}_\ell^T - \sum_{i=1}^{\ell-1} \mathbf{c}_{(\ell, i)} \mathbf{v}_i^T$$

For any arbitrary iteration k and ℓ , residual is of the below form in the DEIM algorithm for the columns of U_1 and U_2 , respectively

$$\begin{aligned} R_k &= (\mathbf{u}_k - \sum_{j=1}^{k-1} \mathbf{c}_{(k, j)} \mathbf{u}_j) \\ R_\ell &= (\mathbf{v}_\ell - \sum_{j=1}^{\ell-1} \mathbf{c}_{(\ell, j)} \mathbf{v}_j) \end{aligned}$$

□

Theorem 2 demonstrates that the new representation of masking operator (P_3, P_4) can be directly derived using Algorithm 2 bypassing the need of TEIM algorithm (TEIM). The results of Theorems 2 and 1 are useful in achieving the objective of approximating the matrix-valued function without transforming it into vectorized form. The following portion of this section outlines the same. In order to achieve this, we have defined a permutation operator, as required in Theorem 3.

Definition 2. A permutation matrix P_{mn} is square $mn \times mn$ matrix partitioned in $m \times n$ sub-matrices such that ij -th sub-matrix has a 1 at the ji -th position and zero elsewhere [22]

$$P_{mn} = \sum_{i=1}^m \sum_{j=1}^n E_{ij} \otimes_k E_{ij}^T$$

Where $E_{ij} = e_i e_j^T = e_i \otimes_k e_j^T$ is the elementary matrix of order $m \times n$, and $e_i(e_j)$ is a column vector with unity in the $i^{th}(j^{th})$ position and zeros elsewhere of order $m \times 1(n \times 1)$.

Theorem 3. Assume the equation (13) of lemma 2 is given and $P = P_{n_1 n_2}$ as per Definition 2 then

$$vec(M(\mathcal{U}X)) = (P^T (P_6 U_2) \otimes_k (P_5 U_1)) vec X$$

and,

$$vec((MU)^{-1} X) = ((P_6 U_2)^{-1} \otimes_k (P_5 U_1)^{-1}) P_{m_2 m_1} vec X$$

where, P_5 and P_6 are the mask operators obtained from algorithm 2.

Proof. Using the mixed product property of Kronecker and Khatri-Rao product [23],

$$(A \otimes_k B)(C \otimes_{kr} D) = AC \otimes_{kr} BD$$

(13) can be written as below

$$\begin{aligned} vec(M(\mathcal{U}X)) &= (U_2^T P_2^T \otimes_{kr} U_1^T P_1^T)^T vec X \\ &= ((U_2^T \otimes_k U_1^T)(P_2^T \otimes_{kr} P_1^T))^T vec X \end{aligned} \quad (24)$$

As $A \otimes_{kr} B$ is the same as $B \otimes_{kr} A$ with few row exchanges for a given A and B of compatible size for Khatri-rao product. Then using the property mentioned in equation 2.14 of [22]

$$P_2^T \otimes_{kr} P_1^T = P_{n_1 n_2} (P_1^T \otimes_{kr} P_2^T) \quad (25)$$

Based on (25), (24) can be represented as,

$$vec(M(\mathcal{U}X)) = ((U_2^T \otimes_k U_1^T) P_{n_1 n_2} (P_1^T \otimes_{kr} P_2^T))^T vec X \quad (26)$$

Using the Lemma 1, (26) reduces to

$$vec(M(\mathcal{U}X)) = ((U_2^T \otimes_k U_1^T) P_{n_1 n_2} (P_3^T \otimes_k P_4^T))^T vec X \quad (27)$$

From equation 3.5, as discussed in [24], $P_{n_1 n_2} (P_3^T \otimes_k P_4^T) P_{m_1 m_2}$ can be written as $P_4^T \otimes_k P_3^T$. And since $P_{m_1 m_2}^{-1} = P_{m_1 m_2}^T = P_{m_2 m_1}$, then (27) can be written as

$$\begin{aligned} vec(M(\mathcal{U}X)) &= ((U_2^T \otimes_k U_1^T) P_{n_1 n_2} (P_3^T \otimes_k P_4^T) \\ &\quad P_{m_1 m_2} P_{m_2 m_1})^T vec X \\ &= ((U_2^T \otimes_k U_1^T) (P_4^T \otimes_k P_3^T) P_{m_2 m_1})^T vec X \\ &= ((U_2^T P_4^T \otimes_k U_1^T P_3^T) P)^T vec X \\ &= (P_{m_2 m_1}^T (P_4 U_2 \otimes_k P_3 U_1)) vec X \end{aligned} \quad (28)$$

Let $M_{uk} = P_{m_2 m_1}^T (P_4 U_2) \otimes_k (P_3 U_1)$. For a given matrix of appropriate dimension,

$$\begin{aligned} vec(X) &= vec((MU)(MU)^{-1} X) = M_{uk} vec((MU)^{-1} X) \\ M_{uk} vec((MU)^{-1} X) &= vec(X) \\ vec((MU)^{-1} X) &= M_{uk}^{-1} vec(X) \\ &= (P_{m_2 m_1}^T (P_4 U_2) \otimes_k (P_3 U_1))^{-1} vec(X) \\ &= ((P_4 U_2) \otimes_k (P_3 U_1))^{-1} P_{m_2 m_1} vec(X) \end{aligned}$$

The existence of the inverse of $((P_4 U_2) \otimes_k (P_3 U_1)) \in \mathbb{R}^{m_1 m_2 \times m_1 m_2}$ implies that the rank of $((P_3 U_1) \otimes_k (P_4 U_2))$ is $m_1 m_2$. Here, $(P_3 U_1) \in \mathbb{R}^{m_1 \times m_1}$ and $(P_4 U_2) \in \mathbb{R}^{m_2 \times m_2}$ can achieve a maximum rank of m_1 and m_2 , respectively. The following conclusion is based on the 4th property of section 2.3 and 3rd property of section 2.5 of [22].

$$vec((MU)^{-1} X) = ((P_4 U_2)^{-1} \otimes_k (P_3 U_1)^{-1}) P_{m_2 m_1} vec(X)$$

Using the Theorem 3,

$$vec((MU)^{-1} X) = ((P_5 U_2)^{-1} \otimes_k (P_6 U_1)^{-1}) P_{m_2 m_1} vec(X)$$

□

3.2 Final Form of Approximated Matrix-valued Function

Using the result of Theorems 3 and (14), $A(t)$ can be approximated as

$$\begin{aligned} \text{vec}(\tilde{A}(t)) &= (U_2 \otimes_k U_1)((P_6 U_2)^{-1} \otimes_k (P_5 U_1)^{-1}) \\ &\quad * \text{vec}(M(A(t))^T) \\ &= (U_2(P_6 U_2)^{-1}) \otimes_k U_1(P_5 U_1)^{-1} \\ &\quad * P_{m_2 m_1} \text{vec}(M(A(t))) \end{aligned}$$

Here, $\text{vec}(M(A(t))) = \text{vecd}(P_1 A(t) P_2^T) = (P_2^T \otimes_{kr} P_1^T)^T \text{vec}(A(t))$. Since $P_{n_1 n_2} (P_5^T \otimes_k P_6^T) P_{m_1 m_2} = P_6^T \otimes_k P_5^T$ and using the Lemma 1, $P_{m_1 m_2} \text{vec}(M(A(t))) = (P_6 \otimes_k P_5) \text{vec}(A(t))$. The resulting expression is reduced to

$$\tilde{A}(t) = U_1(P_5 U_1)^{-1} (P_5 A(t) P_6^T) (U_2(P_6 U_2)^{-1})^T \quad (29)$$

3.3 Computational Complexity

The online computation required to approximate the matrix-valued function depends on the evaluation direction, either from left to right or from right to left. In the former case, it is $\mathcal{O}(n_1 n_2 m_2 + n_1 m_1 m_2)$, while in the latter, it is $\mathcal{O}(n_1 n_2 m_1 + n_2 m_1 m_2)$. The evaluation of $U_1(P_5 U_1)^{-1}$ and $(U_2(P_6 U_2)^{-1})^T$ of dimensions $n_1 \times m_1$ and $n_2 \times m_2$, respectively do not take part in online computation as it is time independent and hence can be computed offline. From Table 3, it can be observed that the approximation of matrix-valued function using P_1 and P_2 requires more computation than that obtained using P_5 and P_6 for $n_1 \gg m_1$ and $n_2 \gg m_2$. If $m_1 < m_2$, then the preferred direction for evaluating the approximated function $\tilde{A}(t)$ is from left to right as it requires less computation compared to other way around (i.e., right to left) and vice-versa. Table 3 also provides an insight into the online computation demands of the DEIM method [15]. The computation is shown corresponding to $m = m_1 m_2$ number of interpolation points for ease of comparison with the proposed method. It can be seen that approximating the matrix-valued function using the DEIM method requires more online computation than the TEIM method (P_5 and P_6) for $n_1 \gg m_1$ and $n_2 \gg m_2$.

3.4 Comparative Analysis of Accuracy: DEIM vs. TEIM

From the discussion of Section 2, the empirical basis of the matrix-valued function can be computed either through the tensor POD method or by transforming the matrix-valued function into a vector-valued function and subsequently calculating the basis using POD method. In this section, we show how the choice of basis affects the approximation of function obtained through the DEIM or TEIM methods. Let $Z = [Z_1 \ Z_2] \in \mathbb{R}^{n_1 \times n_1}$ and $V = [V_1 \ V_2] \in \mathbb{R}^{n_2 \times n_2}$ are the full factor matrices obtained from tensor decomposition. These matrices are used to approximate the $A(t) \in \mathbb{R}^{n_1 \times n_2}$ without any loss. Then, the coefficient corresponding to an orthogonal projection can be written as

$$C = Z^T A(t) V \quad (30)$$

and, $\hat{A}(t) = Z C V^T$. Moreover, from (29), the approximation of $A(t)$ can be written as

$$\begin{aligned} \tilde{A}(t) &= Z_1(P_5 Z_1)^{-1} (P_5 Z C V^T P_6^T) (V_1(P_6 V_1)^{-1})^T \\ &= Z_1(P_5 Z_1)^{-1} P_5 [Z_1 \ Z_2] \begin{bmatrix} C_{11} & C_{12} \\ C_{21} & C_{22} \end{bmatrix} (V_1(P_6 V_1)^{-1} P_6 [V_1 \ V_2])^T \\ &= Z_1(P_5 Z_1)^{-1} [P_5 Z_1 \ P_5 Z_2] \begin{bmatrix} C_{11} & C_{12} \\ C_{21} & C_{22} \end{bmatrix} (V_1(P_6 V_1)^{-1} [P_6 V_1 \ P_6 V_2])^T \\ &= [Z_1 \ Z_1(P_5 Z_1)^{-1} (P_5 Z_2)] \begin{bmatrix} C_{11} & C_{12} \\ C_{21} & C_{22} \end{bmatrix} ([V_1 \ V_1(P_6 V_1)^{-1} (P_6 V_2)])^T \\ &= Z_1 C_{11} V_1^T + Z_1(P_5 Z_1)^{-1} (P_5 Z_2) C_{21} V_1^T + Z_1 C_{12} (V_1(P_6 V_1)^{-1} (P_6 V_2))^T \\ &\quad + Z_1(P_5 Z_1)^{-1} (P_5 Z_2) C_{22} (V_1(P_6 V_1)^{-1} (P_6 V_2))^T \end{aligned} \quad (31)$$

where $Z_1 \in \mathbb{R}^{n_1 \times m_1}$, $Z_2 \in \mathbb{R}^{n_1 \times n_1 - m_1}$, $V_1 \in \mathbb{R}^{n_2 \times m_2}$, $V_2 \in \mathbb{R}^{n_2 \times n_2 - m_2}$ and matrix C is partitioned so as to make it compatible for matrix multiplication.

Similarly, if we approximate the matrix-valued function by transforming it into vector form using the DEIM method, resulting in the below form [51]

$$\text{vec}(\tilde{A}(t)) = \Phi_1 \Phi_1^T \text{vec}(A(t)) + \Phi_1 (P \Phi_1)^{-1} P \Phi_2 \Phi_2^T \text{vec}(A(t)) \quad (32)$$

Masking Operator used in approximation	Online Computation
TEIM method (P_1 and P_2)	$\mathcal{O}(n_1 n_2 m_2 m_1)$
TEIM method (P_5 and P_6)	$\mathcal{O}(n_1 n_2 m_2 + n_1 m_1 m_2)$ or $\mathcal{O}(n_1 n_2 m_1 + n_2 m_1 m_2)$
DEIM method	$\mathcal{O}(n_1 n_2 m_2 m_1)$

Table 3: Computational complexity corresponding to different methods where n_1, n_2 signifies the dimension of original matrix ($A(t)$) and $m_1 m_2$ denote the number of interpolation points ($m_1 \ll n_1$ and $m_2 \ll n_2$) used to approximate the function $A(t)$.

where, $\phi = [\phi_1 \ \phi_2] \in \mathbb{R}^{n_1 n_2 \times n_1 n_2}$ represents the complete POD basis for $\text{vec}(A(t))$ and $P \in \mathbb{R}^{m_1 m_2 \times n_1 n_2}$. The best approximation achievable for a given basis is obtained through the orthogonal projection. The approximated function obtained using the masking operator strives to emulate the outcome of orthogonal projection closely. Nevertheless, the choice of basis leads to distinct approximation via orthogonal projection. Upon examining equations (31) and (32), it can be observed that both the TEIM and DEIM methods involve approximation terms based on orthogonal projection using their respective bases. Specifically, the TEIM method employs orthogonal projection with a tensor basis, while the DEIM method relies on orthogonal projection with the traditional POD basis. Consequently, if the tensor basis offers a more effective approximation subspace compared to the standard POD basis, the TEIM method becomes the preferred choice, and vice-versa.

4 Model Reduction and Numerical Experimentation

In this section, we first show the numerical experimentation result related to the approximation of the matrix-valued function with the proposed method. Later, we show the application of matrix approximation (obtained in Section 3) in the model reduction of semi-linear matrix differential equations and vector differential equations along with their experimental result.

4.1 Approximation of matrix-valued function

This section demonstrates the approximation of the non-linear parameterized 2D function. We applied HOSVD to obtain the empirical basis of the space generated by function evaluated on different parameters (μ) or time (t), whereas the DEIM technique [15] requires the usage of a standard POD basis. The standard POD basis works only for vector-valued functions. In the case of a matrix-valued function, it must be transformed into a vector form for each parameter, thus making the offline and online processes computationally inefficient. Therefore, the function is approximated using (29).

4.1.1 Example 1

The example considered here is adapted from [15]. The function $f: \Omega \times D \rightarrow \mathbb{R}$

$$f(x, y, \mu) = \frac{1}{\sqrt{(x - \mu_1)^2 + (y - \mu_2)^2 + 0.1^2}}$$

where $(x, y) \in \Omega = [0.1, 0.9]^2$ and $\mu = (\mu_1, \mu_2) \in D = [-1, -0.01]^2$. Let (x_i, y_j) be a uniform grid on Ω for $i = 1, \dots, 20$ and $j = 1, \dots, 20$. Let

$$S(\mu) = [\mathbf{f}(x_i, y_j, \mu)] \in \mathbb{R}^{20 \times 20}$$

The POD basis is built using the 225 snapshots created from evenly chosen parameters $\mu_k = (\mu_1^k, \mu_2^k)$ in parameter domain D . The sampled data for different values of μ_k are arranged in the tensor form such that

$$X(:, :, k) = [\mathbf{f}(x_i, y_j, \mu_k)]$$

m	m1	m2	Relative average error with TEIM method	Relative average error with DEIM method	Relative average error with orthogonal projection using tensor bases	Relative average error with orthogonal projection using POD bases
4	2	2	0.005697	$8.14932 * 10^{-04}$	0.002514	$4.08034 * 10^{-04}$
6	3	2	0.001995	$3.28161 * 10^{-04}$	$9.53900 * 10^{-04}$	$1.79717 * 10^{-04}$
8	4	2	0.002044	$2.65126 * 10^{-04}$	$9.49804 * 10^{-04}$	$1.15664 * 10^{-04}$
9	3	3	$1.65512 * 10^{-04}$	$2.34773 * 10^{-04}$	$1.05302 * 10^{-04}$	$1.04193 * 10^{-04}$
12	4	3	$7.12043 * 10^{-05}$	$2.26993 * 10^{-04}$	$4.19038 * 10^{-05}$	$9.58542 * 10^{-05}$
15	5	3	$6.67833 * 10^{-05}$	$2.27548 * 10^{-04}$	$3.97717 * 10^{-05}$	$9.21281 * 10^{-05}$
16	4	4	$3.43754 * 10^{-05}$	$1.86931 * 10^{-04}$	$1.29211 * 10^{-05}$	$9.15026 * 10^{-05}$
20	4	5	$3.42732 * 10^{-05}$	$1.74713 * 10^{-04}$	$1.27067 * 10^{-05}$	$8.87705 * 10^{-05}$
24	4	6	$3.42973 * 10^{-05}$	$1.73714 * 10^{-04}$	$1.27050 * 10^{-05}$	$8.73300 * 10^{-05}$
25	5	5	$8.84877 * 10^{-07}$	$1.70818 * 10^{-04}$	$6.65309 * 10^{-07}$	$8.50820 * 10^{-05}$

Table 4: Relative average norm for TEIM and DEIM methods with varying interpolation points in Example 1. In this context, $m_1 m_2$ represents the number of interpolation points for the TEIM method (where m_1 and m_2 correspond to the selected number of rows and columns), and m denotes the number of interpolation points for the DEIM method.

Here $X \in \mathbb{R}^{20 \times 20 \times 225}$. The first four POD and tensor bases are shown in Figure 1(b) and 1(a), respectively. In order to measure the accuracy, we have used the relative average norm, which is defined as,

$$\xi(f) = \frac{1}{n_\mu} \sum_{i=1}^{n_\mu} \frac{|f(\mu_i) - \hat{f}(\mu_i)|_F}{|f(\mu_i)|_F} \quad (33)$$

To check the accuracy of the approximation with our method TEIM and DEIM [15], the function is approximated for 625 equally spaced parameters $\mu_i = (\mu_1^i, \mu_2^i)$ in domain D, and the results are displayed in Table 4.

As per discussion of Section 3.4, it can be noted that the accuracy of approximations obtained through the DEIM and our proposed TEIM method relies on orthogonal projection. In addition, as we increase the number of interpolation points the approximation error using TEIM or DEIM method approaches to orthogonal projection error [51, 15]. The proposed TEIM method operates on a tensor POD basis, while DEIM operates on a standard POD basis. Table 4 shows that the orthogonal projection error using a tensor POD basis (defined in appendix B for the orthogonal projection method for tensor basis) is less than using a POD basis for nine or more interpolation points. Consequently, the proposed TEIM approximation performs slightly better than the DEIM method. For parameter $\mu = (-0.7879, -0.7171)$, the original and approximated function with TEIM method using 25 interpolation points where $m_1 = 5$ and $m_2 = 5$ is shown in Figure 3. As discussed in Section 3.3, the computational complexity of approximating the matrix-valued function using the DEIM method is more than the TEIM method, which is illustrated by the average computation time graph in Figure 1(b). The average computation graph is plotted over parameter set μ^t (where μ^t contains 625 parameters equally spaced in parameter domain D) for different interpolation points.

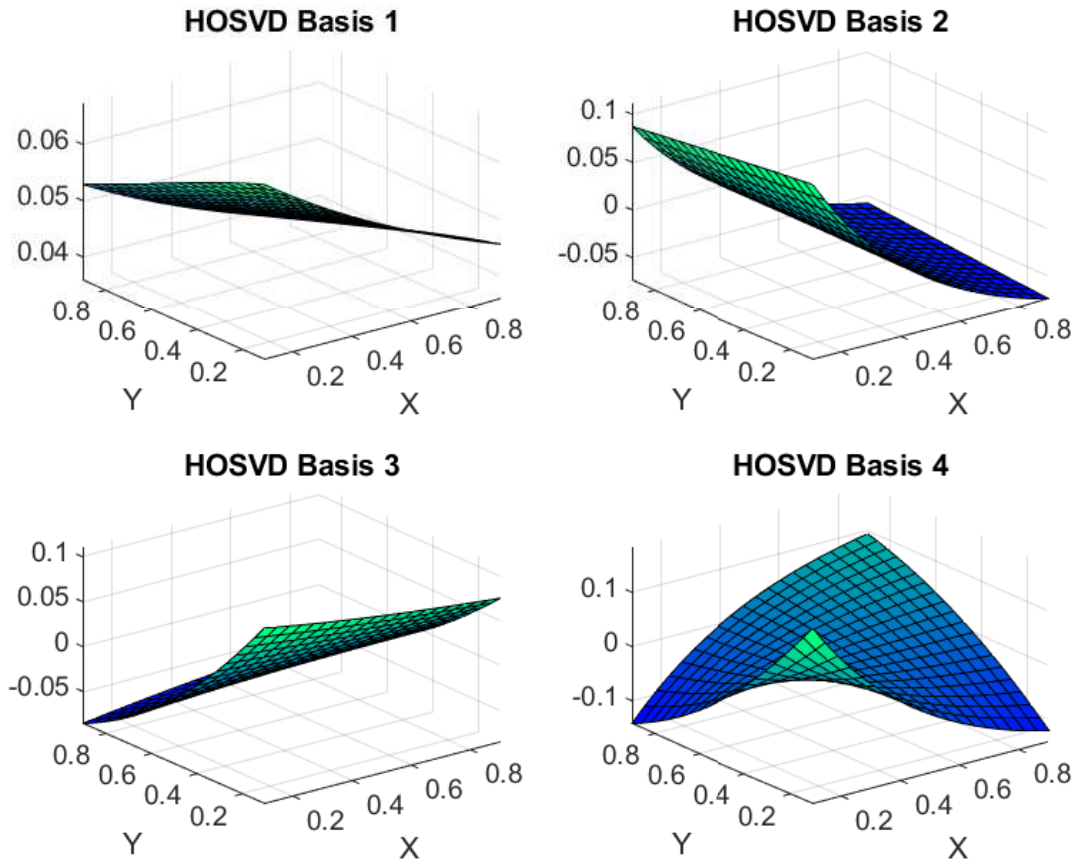
4.1.2 Example 2

This example shows that the DEIM approximation [15] method performs better than the TEIM method, if regular POD bases provide better approximation subspace than tensor POD bases. Suppose \mathbb{P} and \mathbb{P}_T are the orthogonal projection operators for usual and tensor POD bases, respectively. The approximation subspace provided by \mathbb{P} is better than the subspace provided by \mathbb{P}_T , if the average error using projection operator \mathbb{P} is less than the projection operator \mathbb{P}_T .

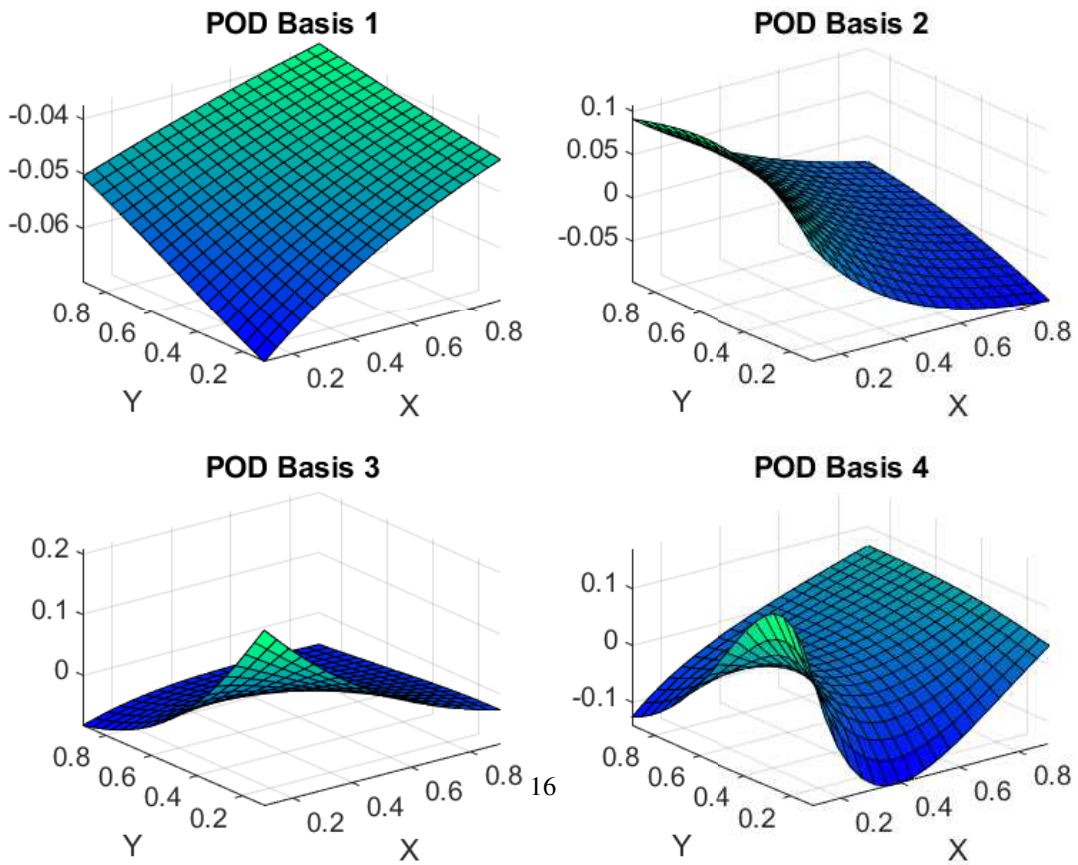
The function $f : \Omega \times [0, T] \rightarrow \mathbb{R}$

$$f(x, y, t) = \frac{1}{\sqrt{(x + y - t)^2 + (2x - 3t)^2 + 0.01^2}}$$

where $(x, y) \in \Omega = [0, 2]^2$ and $T = 2$. Let (x_i, y_j) be a uniform grid on Ω for $i = 1, \dots, 50$ and $j = 1, \dots, 50$. In order to generate the tensor POD bases, the function is evaluated for equally spaced 300 time-steps and arranged into a tensor as described in Section 3. The accuracy result of the DEIM method [15] and the proposed TEIM method is shown in Table 5 for equally spaced 400 time-steps. In Table 5, m denote the number of interpolation points for the DEIM method or the number of POD bases, whereas (m_1, m_2) denotes the number of interpolation points for the TEIM method or the number of tensor POD basis. Figures 4(a) and 4(b) show the first four tensor and usual POD bases, respectively. For parameter, $t = 0.5$, the original and approximated functions with the TEIM method using 49 interpolation points where $m_1 = 7$ and $m_2 = 7$ are shown in Figure 5.



(a) HOSVD Basis



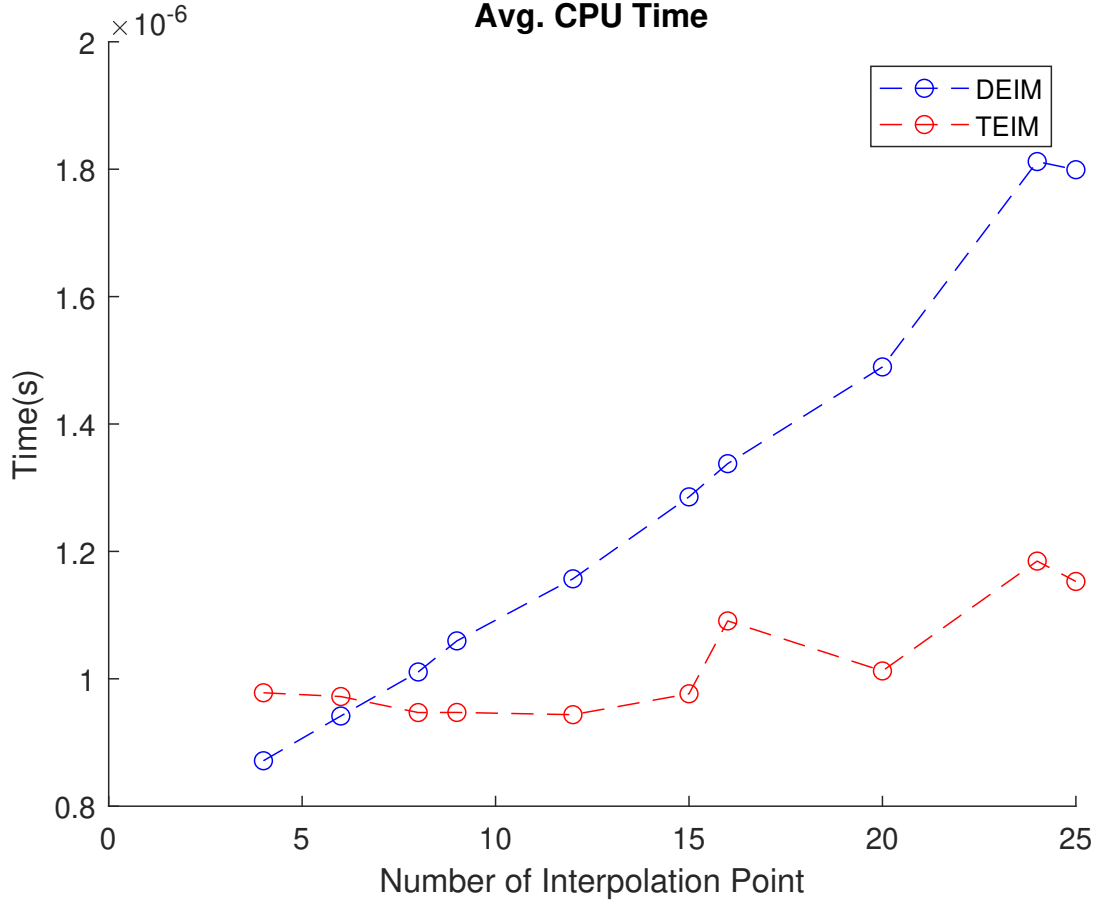


Figure 2: Average Computation Time for a different number of interpolation points.

m	m ₁	m ₂	Relative average error with TEIM method	Relative average error with DEIM method	Relative average error with orthogonal projection using tensor bases	Relative average error with orthogonal projection using POD bases
9	3	3	0.3726	0.2367	0.2378	0.1077
16	4	4	0.2711	0.1083	0.1903	0.0510
15	5	3	0.3293	0.1123	0.2346	0.0569
15	3	5	0.3169	0.1123	0.1586	0.0569
25	5	5	0.2527	0.0657	0.1522	0.0227
36	6	6	0.2169	0.0581	0.1220	0.0109
49	7	7	0.1877	0.0185	0.0986	0.0058
81	9	9	0.1450	0.0025	0.0649	0.0012
121	11	11	0.0802	0.0010	0.0425	1.59*10-04

Table 5: Relative average norm for TEIM and DEIM methods with varying interpolation points in Example 2. In this context, $m_1 m_2$ represents the number of interpolation points for the TEIM method (where m_1 and m_2 correspond to the selected number of rows and columns, respectively.), and m denotes the number of interpolation points for the DEIM method.

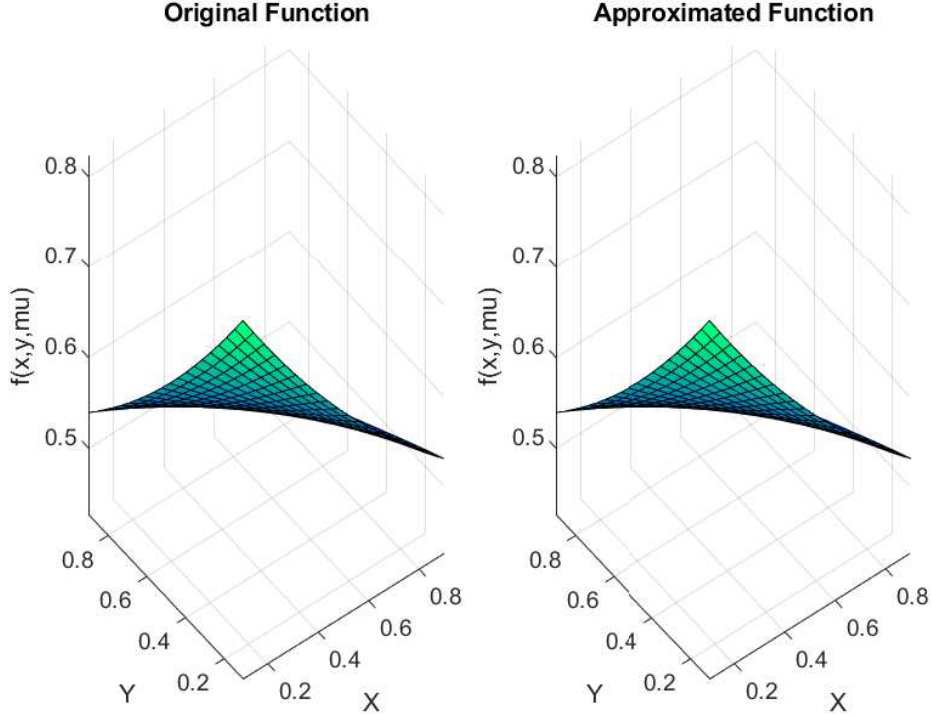


Figure 3: Original and Approximated function for $\mu = (-0.7879, -0.7171)$.

On the basis of accuracy outcomes as observed in Examples 1 and 2, it can be inferred that in cases where tensor POD bases exhibit better approximation subspace compared to conventional POD bases, the TEIM method is preferred over the DEIM method.

4.2 TEIM reduced semi-linear matrix differential equation

The semi-linear matrix differential equation is described as [38]

$$\dot{X}(t) = AX(t) + X(t)B + F(X, t), \quad X(0) = X_0 \quad (34)$$

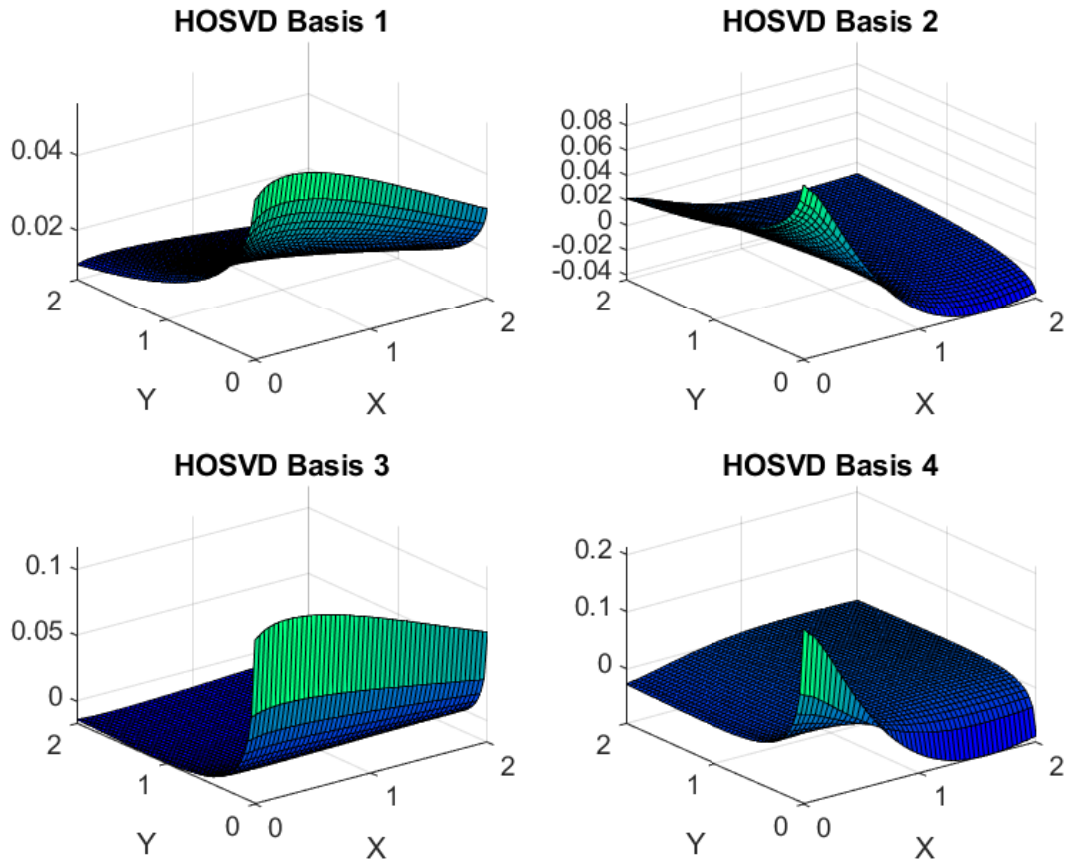
where $X(t) \in S$ (S denote the solution space), $A \in \mathbb{R}^{n_x \times n_x}$, $B \in \mathbb{R}^{n_y \times n_y}$, and $t \in [0, t_f] = T$, given with the appropriate boundary condition. The function $F : S \times T \rightarrow \mathbb{R}^{n_x \times n_y}$ is sufficiently smooth.

By applying the technique outlined in Section 2.1, the appropriate projection space can be formed using the tensor decomposition method. Consider the bases represented as $(v_i^{(1)} \otimes v_j^{(2)})_{i=1, j=1}^{k_1, k_2}$, which constitute the projection space. Here, k_1 and k_2 refer to the number of tensor POD modes. With these tensor bases (tensor POD modes), $X(t)$ can be approximated as $V_1 \tilde{X}(t) V_2^T$ where $V_1 \in \mathbb{R}^{n_x \times k_1}$ and $V_2 \in \mathbb{R}^{n_y \times k_2}$ consist of orthonormal columns $v_i^{(1)}$ and $v_j^{(2)}$, respectively. In the original model, $X(t)$ is substituted with $V_1 \tilde{X}(t) V_2^T$, and this replacement is followed by applying the Galerkin projection condition, which leads to the reduced system given by

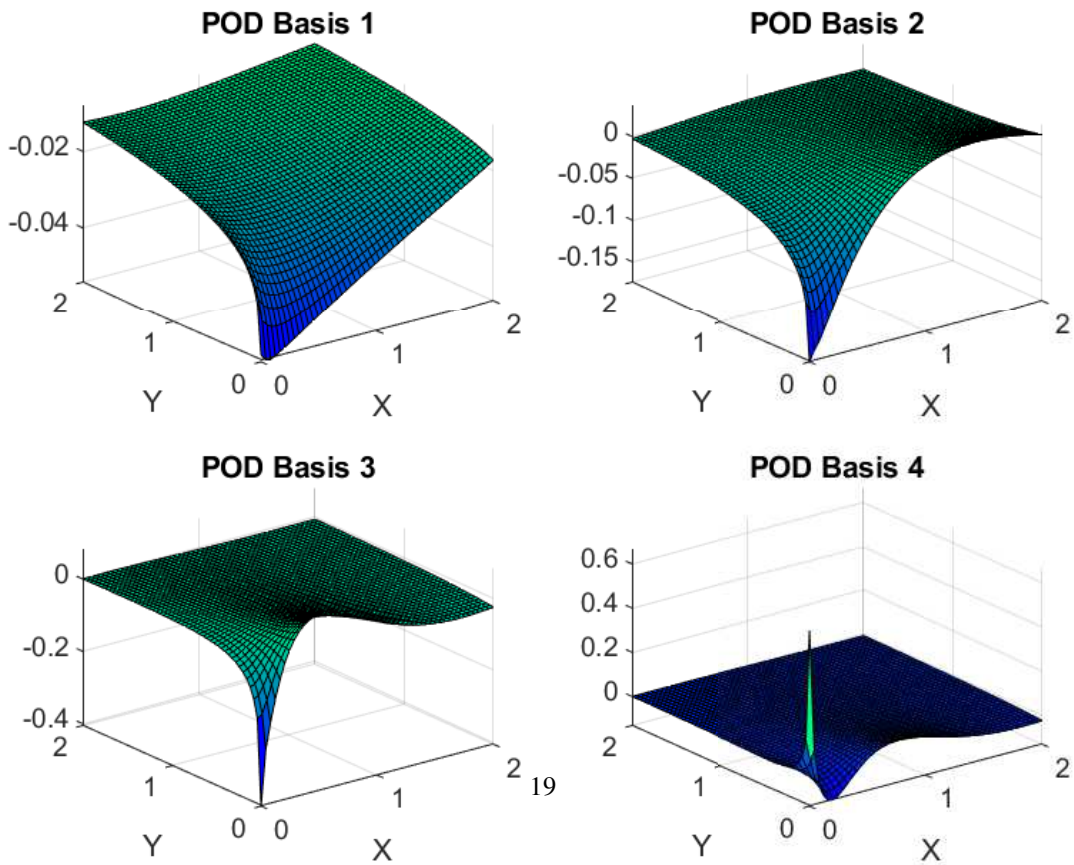
$$\dot{\tilde{X}}(t) = V_1^T A V_1 \tilde{X}(t) + \tilde{X}(t) V_2^T B V_2 + V_1^T F(\tilde{X}, t) V_2$$

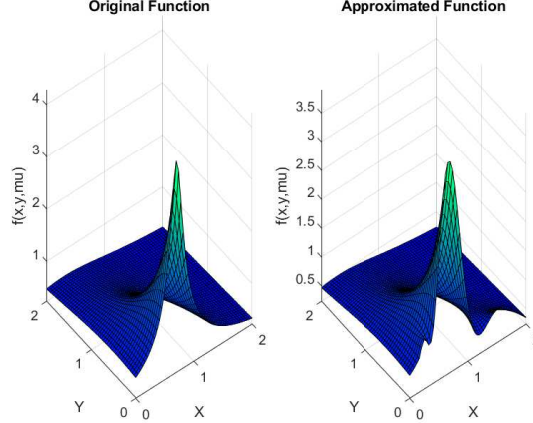
While the system dimension has been reduced from the original $n_1 n_2$ dimensions to $k_1 k_2$ dimensions, it still demands $\mathcal{O}(n_1 n_2)$ computations for evaluating the non-linear term. We have applied the approximation method discussed in Section 3 to mitigate this dependency. Thus, the reduced system is as follows

$$\begin{aligned} \dot{\tilde{X}}(t) = & A_r \tilde{X}(t) + \tilde{X}(t) B_r + V_1^T U_1 (P_3 U_1)^{-1} (P_3 A(t) P_4^T) \\ & (U_2 (P_4 U_2)^{-1})^T V_2 \end{aligned} \quad (35)$$



(a) Tensor Basis



Figure 5: Original and Approximated function for the $t = 0.5$.

where $A_r = V_1^T A V_1 \in \mathbb{R}^{k_1 \times k_1}$, $B_r = V_2^T B V_2 \in \mathbb{R}^{k_2 \times k_2}$, $(v_i^{(1)} \otimes v_j^{(2)})_{i=1, j=1}^{k_1, k_2}$ are the empirical bases where the solution lies approximately at each time-step, and $(u_i^{(1)} \otimes u_j^{(2)})_{i=1, j=1}^{m_1, m_2}$ are the bases of space spanned by $F(X, t)$ for different time-steps.

Table 8 shows offline computation comparison for different methods. This offline computation is required for reducing FOM of dimension $n_1 n_2$ to the reduced model of dimension $k_1 k_2$ using $m_1 m_2$ number of interpolation points. It is evident that the reduction with the proposed method requires less offline computation compared to other methods where we have considered that $n_s > n_1$, $n_s > n_2$, but $n_s < n_1 n_2$ (this assumption is based on fact that, for very large systems, the reduced model should be built with a minimum number of observations. A similar assumption is considered in [15]).

The online computation needed to solve the reduced system (35) with the 4^{th} order Runge-Kutte method at each time-step (modified to solve to matrix differential equation mentioned in (35)) amounts to $\mathcal{O}(k_1^2 k_2 + k_2^2 k_1 + k_1 m_1 m_2 + k_1 k_2 m_2)$ or $\mathcal{O}(k_1^2 k_2 + k_2^2 k_1 + k_2 m_1 m_2 + k_1 k_2 m_1)$ based on the direction of computing the non-linear term present in the reduced system. To compare the online computational complexity with the POD-DEIM reduced system, we assume that $k = k_1 k_2$ (to maintain consistency in the reduced system's dimension using the POD-DEIM and TEIM approaches) and $m = m_1 m_2$ (to keep the number of interpolation points same for both methods). The online computation required to solve POD-DEIM reduced system with the 4^{th} order Runge kutta method at each time-step is $\mathcal{O}(k_1^2 k_2^2 + k_1 k_1 m_1 m_2)$, which is higher than the TEIM reduced system. Table 6 illustrates the online computation required for different methods to solve the reduced system with the Runge Kutta method at each time-step. An important observation is that the mentioned online computation can only be achieved if we solve the (35) in the given matrix form.

In this method of model reduction with TEIM, low dimensional spaces to approximate solution trajectories $X(t)$ and non-linearity present in the dynamical system $F(X(t))$ are constructed through tensor basis. So, this method of model reduction is preferred in cases where tensor POD bases provide a better approximation subspace than the usual POD bases for $X(t)$ and $F(X(t))$. Here, better approximation subspace refers to the subspace where approximation through orthogonal projection leads to less average error or better accuracy compared to other subspaces.

4.2.1 Numerical simulation of model reduction of semi-linear differential equation

We have considered the example of 2D Allen-Cahn equation [38] for model reduction, where the equation of the model is considered as

$$u_t = \epsilon_1 \Delta - \frac{1}{\epsilon_2^2} (u^3 - u), \quad \omega = [0, 2\pi]^2, \quad t \in [0, 5] \quad (36)$$

We have used the same initial condition and parameters, i.e., $u(x, y, 0) = 0.05 \sin x * \cos y$, $\epsilon_1 = 10^{-2}$ and $\epsilon_2 = 1$ as given in [38]. The spatial domain, represented by ω , is discretized into a grid with dimensions of $n_x = 30$ and $n_y = 30$ over the interval $[0, 2\pi]$ in both the x and y directions with the finite-difference method. The resulting ODE system is formed as (34). The model is simulated for 5s with a time-step of 0.025s. To capture the variations robustly, we have applied the tensor POD method to mean subtracted data. As (34) is a matrix differential equation, we employed

Reduction Method	Online Computation
TEIM reduced semi-linear matrix differential equation	$\mathcal{O}(k_1^2 k_2 + k_2^2 k_1 + k_1 m_1 m_2 + k_1 k_2 m_2)$ or $\mathcal{O}(k_1^2 k_2 + k_2^2 k_1 + k_2 m_1 m_2 + k_1 k_2 m_1)$
TEIM reduced vector differential equation	$\mathcal{O}(k_1^2 k_2^2 + k_1 k_2 m_1 m_2)$
POD-DEIM	$\mathcal{O}(k_1^2 k_2^2 + k_1 k_2 m_1 m_2)$

Table 6: Online computation table corresponding to different methods. The mentioned complexity is required to solve the reduced system with the Runge-Kutta method.

k1	k2	m1	m2	k	m	Relative average error using TEIM method	Relative average error using DEIM method
5	5	5	5	25	25	0.001747	$1.89 * 10^{-4}$
5	5	7	7	25	49	0.001216	$1.89 * 10^{-4}$
6	6	5	5	36	25	0.002087	$1.89 * 10^{-4}$
3	3	3	3	9	9	0.009978	$7.28 * 10^{-4}$
4	3	3	3	12	9	0.008602	$2.15 * 10^{-4}$
3	4	3	3	12	9	0.008580	$2.15 * 10^{-4}$
2	6	3	3	12	9	0.026687	$2.15 * 10^{-4}$
7	7	5	5	49	25	0.001904	$1.89 * 10^{-4}$
7	7	7	7	49	49	$2.7486 * 10^{-4}$	$1.89 * 10^{-4}$

Table 7: Relative average error for the reduced system (using the method described in Section 4.2). k_1 and k_2 represent the number of tensor POD modes while m_1, m_2 represent the number of interpolation points. The shown result is obtained by solving the reduced system with 4th order Runge-Kutta method.

the Runge-Kutta method specifically designed for solving such matrix differential equations. To establish a basis for comparison, we applied the Runge-Kutta method to solve the reduced system obtained by employing the POD-DEIM method. Table 7 shows the accuracy corresponding to different values of interpolation points (m_1, m_2) and tensor POD modes (k_1, k_2).

4.3 TEIM reduced vector differential equation

A semi-linear differential equation can also be reduced by arranging $X(t)$ in vector form. Using the property of Kronecker product, the (34) can be written in vector form as follows

$$\text{vec}(\dot{X}(t)) = (I \otimes A + B^T \otimes I) \text{vec}(X(t)) + \text{vec}(F(X, t)) \quad (37)$$

Using the vector POD method [1] and TEIM method, the system (37) can be reduced. Let us assume that the column space of matrix $V \in \mathbb{R}^{n \times k}$ represents the low dimensional space where the state variables can be represented. Then, we can represent

$$x \approx V \hat{x} \approx [v_1 \ v_2 \ v_3 \ \dots \ v_k] \hat{x} \quad (38)$$

where $k \ll n$ denotes the number of POD mode, and $V \in \mathbb{R}^{n \times k}$ is a full column rank matrix. Since approximation of $F(x, t)$ with TEIM method is $\hat{F}(x, t) = U_1(P_3 U_1)^{-1} (P_3 A(t) P_4^T) * (U_2(P_4 U_2)^{-1})^T$ then $\text{vec}(\hat{F}(x, t)) = (U_2(P_4 U_2)^{-1}) \otimes_k (U_1(P_3 U_1)^{-1}) * \text{vec}(P_3 A(t) P_4^T)$. Suppose $\text{vec}(X(t)) = x(t)$ and $(I \otimes A + B^T \otimes I) = A_1$, then using the Galerkin projection and TEIM method, the reduced system is given by

$$\begin{aligned} \dot{\hat{x}}(t) &= V^T A_1 V \hat{x} + V^T (U_2(P_4 U_2)^{-1}) \otimes_k (U_1(P_3 U_1)^{-1}) \\ &\quad (P_4 \otimes_k P_3) \text{vec}(F(V \hat{x})) \end{aligned} \quad (39)$$

Reduction Method	Procedure	Offline Computation
TEIM reduced semi-linear matrix differential equation	Tensor POD basis	$\mathcal{O}(n_1^2 n_2 n_s + n_2^2 n_1 n_s)$
	2D-DEIM method derived from TEIM method	$\mathcal{O}(m_1^4 + m_1 n_1) + \mathcal{O}(m_2^4 + m_2 n_2)$
	$m_1 m_2$ interpolation indices	$\mathcal{O}(n_1^2 k_1 + n_1 k_1^2)$
	Precompute: $A_r = V_1^T A V_1$	$\mathcal{O}(n_2^2 k_2 + n_2 k_2^2)$
	Precompute: $B_r = V_2^T B V_2$	$\mathcal{O}(n_1 k_1 m_1 + m_1^2 n_1 + m_1^3)$
	Precompute: $V_1^T U_1 (P_3 U_1)^{-1}$	$\mathcal{O}(n_2 k_2 m_2 + m_2^2 n_2 + m_2^3)$
TEIM reduced vector differential equation	Tensor POD basis	$\mathcal{O}(n_1^2 n_2 n_s + n_2^2 n_1 n_s)$
	2D-DEIM method derived from TEIM method	$\mathcal{O}(m_1^4 + m_1 n_1) + \mathcal{O}(m_2^4 + m_2 n_2)$
	$m_1 m_2$ interpolation indices	$\mathcal{O}(n_1^2 n_2^2 k_1 k_2 + n_1 n_2 k_1^2 k_2^2)$
	Precompute: $V^T A V$	$\mathcal{O}(n_1 m_1^2 + n_2 m_2^2 + m_1^3 + m_2^3 + n_1 m_1 m_2 n_2 + k_1 k_2 n_1 n_2 m_1 m_2)$
POD_DEIM method	Precompute: $= V^T (U_2 (P_4 U_2)^{-1}) \otimes_k (U_1 (P_3 U_1)^{-1})$	$\mathcal{O}(n_1 n_2 n_s^2)$
	SVD: POD basis	$\mathcal{O}(m_1^2 m_2^2 + m_1 m_2 n_1 n_2)$
	DEIM algorithm: $m_1 m_2$ interpolation indices	$\mathcal{O}(n_1^2 n_2^2 k_1 k_2 + n_1 n_2 k_1^2 k_2^2)$
	Precompute: $V^T A V$	$\mathcal{O}(n_1 n_2 k_1 k_2 m_1 m_2 + m_1^2 m_2^2 n_1 n_2 + m_1^3 m_2^3)$

Table 8: Computational complexity for constructing reduced systems using different methods.

k	m	Relative average error for DEIM method	m1	m2	Relative average error for TEIM method
7	5	0.0046	5	5	0.0031
7	5	0.0046	4	4	0.0156
7	5	0.0046	5	4	0.0085
7	5	0.0046	4	5	0.0085
7	6	0.0014	7	6	0.0024
7	7	$4.6077 * 10^{-4}$	7	7	$7.7324 * 10^{-4}$
8	5	0.0051	5	5	0.0026
8	5	0.0051	4	4	0.0156
8	5	0.0051	5	4	0.0085
8	6	$5.8386 * 10^{-4}$	7	7	$7.6265 * 10^{-4}$
8	7	$4.2818 * 10^{-4}$	7	5	0.0018

Table 9: Relative average norm for a reduced vector-differential system with DEIM and proposed TEIM method (using method described in Section 4.3). k and m represent the number of POD modes and the number of interpolation points of the DEIM method, respectively, whereas m_1, m_2 denotes the number of interpolation points for the TEIM method.

An important observation is that the computation needed at each time-step in solving this reduced system amounts to $\mathcal{O}(k^2 + km_1^2 m_2^2)$, which is equal to the POD-DEIM reduced system if we choose an equal number of interpolation points. The only difference between the POD-DEIM reduced and TEIM reduced systems is the method chosen to approximate the matrix-valued function. So, the preferred method to reduce the system depends on which method approximates the non-linearity better. If the TEIM method approximates it better than the DEIM method, the preferred method is the TEIM method and vice-versa.

4.3.1 Numerical simulation of TEIM Reduced vector differential equation

We have considered the *Allen-Cahn model* with the same parameters and initial condition as described in 4.2.1. The model is discretized in the spatial domain and arranged in the form of a vector differential equation form. For this vector differential equation, we have used the standard POD method [1] for state space approximation, and to compute the non-linear function efficiently, we have used the proposed TEIM method. The reduced system from the proposed method and POD-DEIM is simulated using the ODE45. Table 9 shows the accuracy of the reduced system with our proposed method and state-of-the-art POD-DEIM method [15] corresponding to different numbers of POD mode and interpolation points. The result shows that the reduced system with POD-DEIM method provides better accuracy than the proposed method with equal online computational complexity.

5 Conclusion

In this article, we introduced a theory and algorithm for approximating matrix-valued functions, extending the concepts from the Empirical Interpolation Method (EIM) and Discrete Empirical Interpolation Method (DEIM) to tensor bases.

A deeper analysis reveals that our proposed algorithm generates interpolation points arranged in a rectangular grid. Consequently, the resulting approximation is equivalent to applying the two-sided DEIM method.

The advantage of employing a two-sided DEIM approach or a rectangular grid is the significantly enhanced computational efficiency, which is the highlight of our method. This efficiency improvement is evident in both the offline and online stages of computation, making our approach more efficient compared to the conventional DEIM technique for matrix-valued function approximation and model reduction. We presented a tabular representation of the results to compare computational performance.

Through two illustrative examples of matrix-valued functions, we initially demonstrated that tensor bases may yield a superior approximation subspace to conventional POD bases. This observation indirectly suggests that the Tensor Empirical Interpolation Method (TEIM) can offer enhanced accuracy relative to the DEIM method in such scenarios. Subsequently, we showcased the application of our proposed method in model reduction through two distinct approaches. Notably, the proposed method requires fewer computational resources but provides a slightly lower level of accuracy when compared to the DEIM method for the given model. This discrepancy arises because conventional POD bases generally offer a more effective subspace than tensor bases.

However, it is essential to recognize that the presented method has the potential to deliver superior accuracy along with reduced computational resources. This advantage becomes particularly apparent in dynamical systems where tensor bases outperform traditional POD bases in terms of defining a suitable approximation subspace.

Although this study is exclusively for matrix-valued functions, it can be extended to tensor-valued ones.

A DEIM Algorithm

In this section, we have provided the DEIM algorithm [15], which is a sub-part of Algorithm 2.

norelsize 3 DEIM

```

Input  $U^T = [u_1 \quad u_2 \dots u_{m_1}], P = 0$ 
Output  $P, \phi$ 
 $[\rho], \phi_1 = \max(|u_1|)$ 
 $P = [e_{\phi_1}], U_1 = [u_1], \phi = [\phi_1]$ 
for  $l = 2, \dots, m_1$  do
    Solve  $(P^T U)c = P^T u_l$ 
     $r = u_l - Uc$ 
     $[\rho], \phi_l = \max(|r|)$ 
     $P_1 = [P_1 \quad e_{\phi_l}], U_1 = [U_1 \quad u_l], \phi = \begin{bmatrix} \phi \\ \phi_l \end{bmatrix}$ 
end for
return  $P, \phi$ 

```

B Approximation of matrix-valued function using orthogonal projection

In this section, we describe the orthogonal projection method using the tensor basis. The approximation of $A(t) \in \mathbb{R}^{n_1 \times n_2}$ through the orthogonal projection technique on the basis $\{u_i \otimes v_j\}_{i=1, j=1}^{m_1, m_2}$ is given by

$$\hat{A}(t) = UU^T A(t) V^T V \quad (40)$$

where, $U = [u_1 \quad u_2 \quad \dots \quad u_{m_1}]$ and $V = [v_1 \quad v_2 \quad \dots \quad v_{m_2}]$.

Similarly, the approximation of $f(t) \in \mathbb{R}^{n_1 n_2}$ ($f(t) = \text{vec}A(t)$) through orthogonal projection on the POD basis $\{z_i\}_{i=1}^{m_1 m_2}$ is given by

$$\hat{f}(t) = ZZ^T f(t) \quad (41)$$

where, $Z = [z_1 \quad z_2 \quad \dots \quad z_{m_1 m_2}]$

References

- [1] Antoulas, A. Approximation of Large-Scale Dynamical Systems. (SIAM, 2005)
- [2] Khalid, R. & Javaid, N. A survey on hyperparameters optimization algorithms of forecasting models in smart grid. *Sustainable Cities And Society*. **61** pp. 102275 (2020)

- [3] Snowden, T., Graaf, P. & Tindall, M. Methods of model reduction for large-scale biological systems: a survey of current methods and trends. *Bulletin Of Mathematical Biology*. **79**, 1449-1486 (2017)
- [4] Bai, Z. Krylov subspace techniques for reduced-order modeling of large-scale dynamical systems. *Applied Numerical Mathematics*. **43**, 9-44 (2002)
- [5] Freund, R. Model reduction methods based on Krylov subspaces. *Acta Numerica*. **12** pp. 267-319 (2003)
- [6] Mullis, C. & Roberts, R. Synthesis of minimum roundoff noise fixed point digital filters. *IEEE Transactions On Circuits And Systems*. **23**, 551-562 (1976)
- [7] Moore, B. Principal component analysis in linear systems: Controllability, observability, and model reduction. *IEEE Transactions On Automatic Control*. **26**, 17-32 (1981)
- [8] Lumley, J. The structure of inhomogeneous turbulent flows. *Atmospheric Turbulence And Radio Wave Propagation*. (1967)
- [9] Hotelling, H. Analysis of a complex of statistical variables into principal components. *Journal Of Educational Psychology*. **24** (1933)
- [10] Galbally, D. Nonlinear model reduction for uncertainty quantification in large-scale inverse problems: application to nonlinear convection-diffusion-reaction equation. (Massachusetts Institute of Technology, 2008)
- [11] Carlberg, K., Farhat, C., Cortial, J. & Amsallem, D. The GNAT method for nonlinear model reduction: effective implementation and application to computational fluid dynamics and turbulent flows. *Journal Of Computational Physics*. **242** pp. 623-647 (2013)
- [12] Everson, R. & Sirovich, L. Karhunen-Loeve procedure for gappy data. *JOSA A*. **12**, 1657-1664 (1995)
- [13] Astrid, P., Weiland, S., Willcox, K. & Backx, T. Missing point estimation in models described by proper orthogonal decomposition. *2004 43rd IEEE Conference On Decision And Control (CDC) (IEEE Cat. No.04CH37601)*. **2** (2004)
- [14] Barrault, M., Nguyen, C., Patera, A. & Maday, Y. An ‘empirical interpolation’ method: application to efficient reduced-basis discretization of partial differential equations. *Comptes Rendus De L’Académie Des Sciences. Série I, Mathématique*. **339-9** pp. 667-672 (2004)
- [15] Chaturantabut, S. & Sorensen, D. Discrete Empirical Interpolation for nonlinear model reduction. *Proceedings Of The 48th IEEE Conference On Decision And Control (CDC) Held Jointly With 2009 28th Chinese Control Conference*. pp. 4316-4321 (2009)
- [16] Huang, Y. & Jadbabaie, A. Nonlinear H_{∞} control: an enhanced quasi-LPV approach. *IFAC Proceedings Volumes*. **32**, 2754-2759 (1999), 14th IFAC World Congress 1999, Beijing, China, 5-9 July
- [17] Drmac, Z. & Gugercin, S. A new selection operator for the discrete empirical interpolation method—improved a priori error bound and extensions. *SIAM Journal On Scientific Computing*. **38**, A631-A648 (2016)
- [18] Peherstorfer, B., Butnaru, D., Willcox, K. & Bungartz, H. Localized discrete empirical interpolation method. *SIAM Journal On Scientific Computing*. **36**, A168-A192 (2014)
- [19] Negri, F., Manzoni, A. & Amsallem, D. Efficient model reduction of parametrized systems by matrix discrete empirical interpolation. *Journal Of Computational Physics*. **303** pp. 431-454 (2015)
- [20] Peherstorfer, B. Model reduction for transport-dominated problems via online adaptive bases and adaptive sampling. *SIAM Journal On Scientific Computing*. **42**, A2803-A2836 (2020)
- [21] Peherstorfer, B. & Willcox, K. Online adaptive model reduction for nonlinear systems via low-rank updates. *SIAM Journal On Scientific Computing*. **37**, A2123-A2150 (2015)
- [22] Langville, A. & Stewart, W. The Kronecker Product and Stochastic Automata Networks. *J. Comput. Appl. Math.*. **167** pp. 429-447 (2004,6)
- [23] C. Radhakrishna Rao Estimation of Heteroscedastic Variances in Linear Models. *Journal Of The American Statistical Association*. **65**, 161-172 (1970)
- [24] Al Zhour, Z. & Kiliçman, A. Some new connections between matrix products for partitioned and non-partitioned matrices. *Computers & Mathematics With Applications*. **54**, 763-784 (2007)
- [25] Rozza, G., Huynh, D. & Patera, A. Reduced Basis Approximation and a Posteriori Error Estimation for Affinely Parametrized Elliptic Coercive Partial Differential Equations. *Archives Of Computational Methods In Engineering*. **15**, 229 - 275 (2008)
- [26] Antoulas, A., Beattie, C. & Güğercin, S. Interpolatory methods for model reduction. (SIAM, 2020)

- [27] Benner, P., Gugercin, S. & Willcox, K. A survey of projection-based model reduction methods for parametric dynamical systems. *SIAM Review*. **57**, 483-531 (2015)
- [28] Antoulas, A., Beattie, C. & Gugercin, S. Interpolatory model reduction of large-scale dynamical systems. *Efficient Modeling And Control Of Large-scale Systems*. pp. 3-58 (2010)
- [29] Saibaba, A. Randomized discrete empirical interpolation method for nonlinear model reduction. *SIAM Journal On Scientific Computing*. **42**, A1582-A1608 (2020)
- [30] Dedden, R. Model order reduction using the discrete empirical interpolation method. (2012)
- [31] Shekhawat, H. & Weiland, S. A Locally Convergent Jacobi Iteration for the Tensor Singular Value Problem. *Multidimensional System Signal Process.*. (2018)
- [32] De Lathauwer, L. Signal processing based on multilinear algebra. (Katholieke Universiteit Leuven Leuven, 1997)
- [33] Loan, C. & Pitsianis, N. Approximation with Kronecker Products. *Linear Algebra For Large Scale And Real-Time Applications*. pp. 293-314 (1993)
- [34] Kreyszig, E. Introductory functional analysis with applications. (John Wiley & Sons, 1991)
- [35] Rynne, B. & Youngson, M. Linear functional analysis. (Springer Science & Business Media, 2007)
- [36] Boyd, S., Boyd, S. & Vandenberghe, L. Convex optimization. (Cambridge university press, 2004)
- [37] Ali Eshtewy, N. & Scholz, L. Model reduction for kinetic models of biological systems. *Symmetry*. **12**, 863 (2020)
- [38] Kirsten, G. & Simoncini, V. A matrix-oriented POD-DEIM algorithm applied to semilinear matrix differential equations. (arXiv, 2020)
- [39] Rowley, C. & Dawson, S. Model Reduction for Flow Analysis and Control. *Annual Review Of Fluid Mechanics*. **49**, 387-417 (2017)
- [40] Wirtz, D., Sorensen, D. & Haasdonk, B. A posteriori error estimation for DEIM reduced nonlinear dynamical systems. *SIAM Journal On Scientific Computing*. **36**, A311-A338 (2014)
- [41] Carlberg, K. Model reduction of nonlinear mechanical systems via optimal projection and tensor approximation. (Stanford University, 2011)
- [42] Kolda, T. & Bader, B. Tensor Decompositions and Applications. *SIAM Rev.* **51** pp. 455-500 (2009)
- [43] Kirsten, G. Multilinear POD-DEIM model reduction for 2D and 3D semilinear systems of differential equations. *Journal Of Computational Dynamics*. **9** pp. 159-183 (2022)
- [44] Choi, Y., Brown, P., Arrighi, W., Anderson, R. & Huynh, K. Space-time reduced order model for large-scale linear dynamical systems with application to Boltzmann transport problems. *Journal Of Computational Physics*. **424** pp. 109845 (2021)
- [45] McBane, S., Choi, Y. & Willcox, K. Stress-constrained topology optimization of lattice-like structures using component-wise reduced order models. *Computer Methods In Applied Mechanics And Engineering*. **400** pp. 115525 (2022), <https://www.sciencedirect.com/science/article/pii/S0045782522005266>
- [46] Cheung, S., Choi, Y., Springer, H. & Kadeethum, T. Data-scarce surrogate modeling of shock-induced pore collapse process. *ArXiv Preprint arXiv:2306.00184*. (2023)
- [47] Kadeethum, T., Jakeman, J., Choi, Y., Bouklas, N. & Yoon, H. Epistemic Uncertainty-Aware Barlow Twins Reduced Order Modeling for Nonlinear Contact Problems. *IEEE Access*. **11** pp. 62970-62985 (2023)
- [48] Yano, M. & Patera, A. An LP empirical quadrature procedure for reduced basis treatment of parametrized nonlinear PDEs. *Computer Methods In Applied Mechanics And Engineering*. **344** pp. 1104-1123 (2019), <https://www.sciencedirect.com/science/article/pii/S0045782518301087>
- [49] Lauzon, J., Cheung, S., Shin, Y., Choi, Y., Copeland, D. & Huynh, K. S-OPT: A points selection algorithm for hyper-reduction in reduced order models. *ArXiv Preprint arXiv:2203.16494*. (2022)
- [50] Zhang, D. & Zhou, Z. (2D)2PCA: Two-directional two-dimensional PCA for efficient face representation and recognition. *Neurocomputing.*, <https://www.sciencedirect.com/science/article/pii/S0925231205001785>, Neural Networks in Signal Processing
- [51] Tripathi, B. & Shekhawat, H. Model Reduction of Large Scale Dynamical System with a Selection of States. *SSRN*.
- [52] D. Bertsekas, *Nonlinear Programming*, 2nd ed. Athena Scientific, 1999, vol. 4.

This figure "test.png" is available in "png" format from:

<http://arxiv.org/ps/2410.21770v1>